



Jani Kuniala

FATIGUE ANALYSIS OF 3-DIMENSIONAL SHIP STRUCTURAL DETAIL

Thesis submitted in partial fulfilment of the
requirements for the degree of Master of
Science in Technology

Espoo, Finland 28.11.2016

Supervisor: Professor Heikki Remes
Advisor: Timo Mikkola, D.Sc (Tech.)
Ingrit Lillemäe, D.Sc (Tech.)

Author Jani Kuniala

Title of thesis Fatigue analysis of 3-dimensional ship structural detail

Degree programme Mechanical Engineering

Major Marine Technology

Code K3005

Thesis supervisor Heikki Remes, Prof.

Thesis advisor(s) Timo Mikkola, D.Sc (Tech.), Ingrid Lillemäe, D.Sc (Tech.)

Date 28.11.2016

Number of pages 68+4

Language English

Abstract

Fatigue assessment is an essential part of ship's structural design process. Classification societies require that the strength of ship structures is verified by the means of finite element method (FEM). Industry standard is to use the shell models in FEM. In case of complex 3-dimensional ship structural details, fatigue damage is often over estimated in numerical analysis, while no fatigue cracks have been found during inspection. One reason for error in numerical analysis might be shell models, which cannot describe the geometry and stiffness of a complex structural detail correctly. Also the weld is not modeled accurately. With solid FE models the geometry and stiffness of structure including the weld can be presented more accurately. This thesis investigates the suitability of solid elements for modeling the lug plate connection of a floating production storage and offloading (FPSO) vessel conversion project. The stress and deformation response as well as fatigue damage of shell and solid element models are compared.

Fatigue is very local phenomenon and ships are large and complex structures. Thus in case of ships structure evaluation, the sub-modeling technique is used to calculate realistic stress response of the lug plate. Both shell and different solid element sub-models are utilized. The fatigue load analysis is performed using spectral analysis. Spectral method is required in case of FPSO conversion, because it is able to take realistic environmental loads into account. The fatigue stress response of the structure is calculated with two different structural hot spot stress methods: through thickness linearization and extrapolation. Extrapolation based on selected distances from the weld is currently recommended by Classification Societies for shell models, while through thickness linearization is independent of the extrapolation points because it is calculated at weld toe. The through-thickness linearization method is only suitable for solid models. In fatigue damage calculation the Palmgren-Miner rule is used with S-N curves.

The extrapolated structural hot spot stress of the densely meshed solid model is clearly lower compared to the shell model. When solid model is constructed of 2 element layers, the stress is only slightly smaller than in the shell model. The difference on hot spot stresses between sparse and dense solid models is partly due to stiffness. Different weld modeling approaches affected to hot spot stress and stiffness results. The shell element model cannot describe bending behavior at the weld toe. This is due to offset element in shell FE model. Farther than one-time thickness of the plate from the weld toe, the bending and normal stresses start to correlate between different models. In fatigue damage level, the denser solid model gives the lowest damage and the results are more in line with the inspections of the FPSO where fatigue cracks were not found. However, the results of the thesis should be validated with full-scale fatigue tests.

Keywords Fatigue, structural hot spot stress, spectral method, lug plate, solid modeling, finite element method, sub-modeling

Tekijä Jani Kuniala

Työn nimi Kolmiulotteisen laivarakenteen väsymisanalyysi

Koulutusohjelma Konetekniikka

Pääaine Meritekniikka

Koodi K3005

Työn valvoja Prof. Heikki Remes

Työn ohjaaja(t) TkT Timo Mikkola, TkT Ingrid Lillemäe

Päivämäärä 28.11.2016

Sivumäärä 68+4

Kieli englanti

Tiivistelmä

Väsymismitoitus on keskeinen osa laivan rakennesuunnittelua. Luokituslaitokset vaativat, että laivan rakenteiden lujuus varmennetaan elementtimenetelmällä. Alan standardina on käyttää kuorimalleja elementtimenetelmässä. Monimutkaisten kolmiulotteisten laivarakenteiden kohdalla väsymisvaurio on usein yliarvioitu numeerisessa laskennassa, vaikka väsymismurtumia ei ole löydetty tarkastusten yhteydessä. Yksi syy virheeseen numeerisessa analyysissä voi olla kuorimallit, jotka eivät pysty kuvailemaan monimutkaisen rakennekappaleen geometriaa ja jäykkyyttä oikein. Lisäksi hitsiä ei ole mallinnettu oikein. Kolmiulotteisilla elementtimalleilla rakenteen geometria ja jäykkyys sisältäen hitsin vaikutus voidaan ottaa tarkemmin huomioon. Tämä opinnäyte tutkii kolmiulotteisten elementtien soveltuvuutta korvake levyn mallintamisessa FPSO laivan konversioprojektissa. Kuori- ja kolmiulotteisten-elementtimallien jännitys- ja muodonmuutosvastetta sekä väsymisvauriota verrataan toisiinsa.

Väsyminen on hyvin paikallinen ilmiö ja toisaalta laivat ovat suuria ja rakenteeltaan monimutkaisia. Näin ollen laivan rakenteiden arvioinnissa alimalleja käytetään korvakelevyn todenmukaisen jännitysvasteen laskemiseen. Alimalleina käytetään sekä kuori- että kolmiulotteisia-elementtimalleja. Väsymiskuorma analyysissä käytetään spektrimenetelmää. FPSO konversioissa vaaditaan spektrimenetelmän käyttöä, koska sen avulla ympäristön aiheuttamat kuormat voidaan realistisemmin ottaa huomioon. Väsymisjännityksen vaste lasketaan kahdella eri menetelmällä: paksuuden yli linearisoimalla ja ekstrapoloimalla. Kuorimalleille ekstrapolointia valituilta etäisyyksiltä suositellaan luokituslaitoksien toimesta, kun taas linearisointi on riippumaton ekstrapolointi pisteistä, koska se lasketaan hitsin ulkoreunalla. Paksuuden yli linearisointi menetelmä on soveltuva ainoastaan kolmiulotteisille-elementtimalleille. Väsymisvaurion laskennassa käytetään Palmgren-Miner sääntöä ja S-N käyriä.

Tiheämmin verkotetun kolmiulotteisenmallin ekstrapoloitu rakenteellinen jännitys on selkeästi pienempi kuorimalliin verrattuna. Kahden elementtitason kolmiulotteisenmallin jännitys on vain hieman pienempi kuin kuorimallin. Ero rakenteellisessa jännityksessä harvan ja tiheän kolmiulotteisenmallin välillä johtuu osittain jäykkyydestä. Erilaiset hitsin mallintamistavat vaikuttivat rakenteelliseen jännitykseen ja jäykkyyteen. Kuorimalli ei pysty kuvaamaan taivutusta hitsin reunalla. Tämä johtuu käytetystä 'offset' elementistä kuorimallissa. Kauempana kuin yhden levynpaksuuden matkaisella mitalla hitsin reunasta, taivutus- ja normaalijännitys alkavat korreloida eri mallien välillä. Väsymisvaurion tasolla tarkasteltuna tiheämpi kolmiulotteinen malli antaa pienimmän vauriosuhteen ja tulokset ovat enemmän linjassa FPSO:lla suoritettujen tarkastuksien kanssa, joissa ei ole löytynyt väsymismurtumia. Toisaalta, opinnäytteen tulokset täytyisi vahvistaa tädenmittakaavan väsymismallikokeissa.

Avainsanat Väsyminen, rakenteellinen jännitys, spektrimenetelmä, korvake levy, kolmiulotteinen mallintaminen, elementtimenetelmä, alimallinnus

Preface

This thesis was carried out as a part of FIMECC BSA – “Breakthrough Steel and Applications” project. Thesis was written at Deltamarin Ltd premises by its funding. The funding is highly appreciated.

I would like to thank my supervisor, Professor Heikki Remes for his guiding, interest towards my topic and patience during this long path. I would like to thank my advisor Ingrid Lillemäe for sharing her knowledge of the topic and guiding in writing process. I also would like to express my deepest gratitude to my advisor Timo Mikkola giving me this interesting topic, being my support the whole process, guiding and sharing his knowledge. I would like to thank my colleague Risto Juujärvi for guiding me in FE modelling.

I wish to thank all my colleagues at Deltamarin office for great atmosphere and support. I would like to thank my manager Johan Hellman giving me time to finalize this thesis.

I would like to express my thanks to my friends and guys from LRK. You made my study time unforgettable. Finally, I would like to thank my family for providing me solid background and being support in my life. Special thanks to my father for showing me that you can achieve wonderful things in life just being determined and enthusiastic.

Helsinki 28.11.2016

Jani Kuniala

Table of content

Abstract	
Preface	
Table of content	i
Symbols	iii
Abbreviations	iv
1 Introduction	1
1.1 Problem background	1
1.2 Research questions	2
1.3 Limitations	3
1.4 Methodology	4
2 State of the art	6
2.1 Wöhler diagram	6
2.1.1 Adaptions of S-N curve based on fatigue analysis	7
2.2 Fatigue stress analysis	8
2.2.1 Nominal stress approach	8
2.2.2 Structural hot spot stress approach	9
2.2.3 Notch stress approach	12
2.3 Effect of modeled weld	13
2.4 The determination of three dimensional structure	13
2.5 Fatigue load analysis and linear damage model	14
2.5.1 Spectral analysis	15
2.5.2 Damage model	16
3 Methods	18
3.1 Sub-modeling	18
3.2 Solid modeling	20
3.3 Derivation of hot spot stress	22
3.3.1 Extrapolation procedure	22
3.3.2 Through thickness linearization and stress field	24
3.3.3 Bending reduction	25
3.4 Fatigue assessment	26
4 Case description	29
4.1 General	29

4.2	Model description.....	31
4.2.1	General	31
4.2.2	Model hierarchy	31
4.2.3	Shell models	33
4.2.4	Solid models.....	34
4.2.5	Loads and boundary conditions	36
4.3	Hot spot locations	38
5	Results.....	40
5.1	Fatigue damage.....	40
5.2	Deformation and stress response of the lug plate connection	43
5.3	Structural hot spot stresses	49
5.4	Through thickness stress distribution	53
5.5	Membrane and bending stress	55
6	Discussion	58
7	Conclusions.....	62
8	Future work and recommendations.....	64
	References	65
	List of appendices	

Symbols

Notations

A	fatigue constant
D	fatigue damage ratio
N	cycles to failure
RF	wetted surface reduction factor
S_{ij}	stress component of stress tensor in ij Cartesian co-ordinate system
T	thickness of plate
X, Y, Z	global co-ordinates
l	length of element
m	slope of S - N curve
n	number of cycles
p	external water pressure
s	stress range
t	thickness of plate or finite element
w	width of element
x, y, z	local co-ordinates
σ	stress

Sub-indexes

i	stress block
mem	membrane
ben	bending
nlp	non-linear stress peak
top	top surface of plate/element
$bottom$	bottom surface of plate/element
e	notch
hs	hot spot
n	nominal
x, y, z	local co-ordinate

Abbreviations

ABS	American Bureau of Shipping
BR	Bending reduction
CSR	Common structural rules
DNV	Det Norske Veritas
DOF	Degrees of freedom
EWP	External wave pressure
FAT	Fatigue design class
FEA	Finite Element Analysis
FEM	Finite Element Method
FPSO	Floating Production Storage and Offloading
HC	High-cycle
HS	Hot Spot
IACS	International Association of Classification Societies
IIW	International Institute of Welding
ISSC	International Ship and Offshore Structures Congress
LC	Low-cycle
MPC	Multipoint constraint
PSCM	Perpendicular shell coupling method
RAO	Response amplitude operator
ROP	Read-Out-Point
SCF	Stress concentration factor
SIF	Stress intensity factor
SRF	Stress response factor
UHC	Ultra-high-cycle

1 Introduction

1.1 Problem background

Fatigue is a local phenomenon caused by cyclic fluctuating stresses (e.g. Hughes and Paik 2010 p. 17-1). Fatigue loads are mainly generated from environmental forces in case of floating vessels. In addition to local loads, the global loads affect the fatigue strength of ships and offshore structures significantly. Therefore, the fatigue strength assessment of ship structural details is very complex. If the fatigue assessment needs to be done in detailed level, the load analysis is done using the spectral method (e.g. Det Norske Veritas 2010).

The floating production, storage and offloading ships (FPSOs) are a special case where fatigue is governing in the design, because these ships are typically operating continuously 20-25 years without dry-docking (Lotsberg 2007). Thus, the inspection and repair work of fatigue cracks is challenging. An interruption in production due to repair work causes an additional economic loss. Therefore, the fatigue assessment of FPSOs is crucial.

In engineering practices, the fatigue strength is defined with $S-N$ curves, which are based on the small-scale tests (e.g. Fricke 2015). The $S-N$ curves can be characterized with three different stress methods: nominal stress, structural hot spot stress and notch stress. At weld toe the stresses are multi-axial in nature, but often single stress component is enough to describe the fatigue stress (Radaj et al. 2009, Chattopadhyay 2011). Thus, the $S-N$ curve with the relevant characterized stress is, at least in principal, a proper way to describe the stress increase at the hot spot. The nominal stress approach requires the least and notch stress the most modeling effort (Horn et al. 2012).

Because of complex structural topology of ship structures, the finite element method (FEM) is a main tool in evaluating stresses for fatigue analysis. The rule based shell modeling has been found unsuitable in fatigue assessment procedure to certain structural details, such as lug plates, brackets and scallop corners. The analysis shows high fatigue damage, but extensive use of these details in practice suggests that the result is overly conservative. These '3 dimensional' details are affected by high local bending due to shear (Fricke and Paetzoldt 1995, Lotsberg 2006). Current design method proposed by classification societies is based on shell or plate elements model, which does not include

the weld (e.g. Det Norske Veritas 2010). However, fatigue is very local phenomenon and the proper weld stiffness affects the results significantly (Chattopadhyay 2011). The shell element simplifies the geometry to mid-planes and in some cases the structural offsets between plates are difficult to model and cause additional stress singularities. The weld can be presented with three different methods (Aygül 2012): rigid links, bar elements and shell elements. The methods are presented in Figure 1. Another approach is to model the problem with solid elements, which can take the local geometry and stiffness into account properly (Goyal 2015). The stresses obtained from solid models have been found to correspond better with the actual stresses of experimental tests (Horn et al. 2009). Lotsberg (2005) found that certain type of lug plate connection modeled with solid elements is in better agreement with experimental tests. The reason was assumed to be the correctly modeled stiffness of the longitudinal due to solid elements. Wang (2008) also studied the lug plate connection and recommended to use solid elements. However, he did not present detailed stress and deformation response on webframe in way of lug plate's hot spot but indicated that longer fatigue lives could be reached with solid elements.

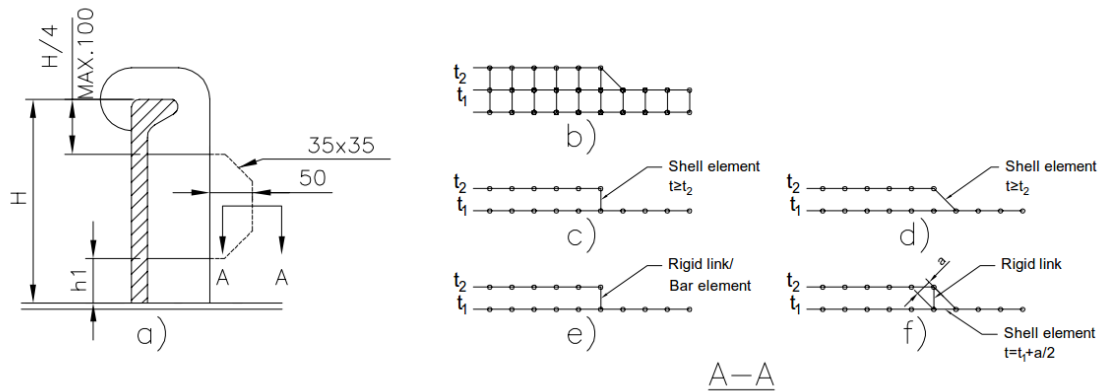


Figure 1. An example of lug plate connection (a) and different modeling techniques of connection: b) solid elements, c) shell element, d) oblique shell element, e) rigid link and f) rigid link with thicker shell element next to offset.

1.2 Research questions

Current design method proposed by classification societies is based on shell or plate elements. The most common practice is to model the structure without the weld. Stresses at the weld toe are multiaxial, but in simple cases one stress component is dominant and enough for fatigue analysis. The structural hot spot stress is in many cases suitable and accurate enough to define stresses based on macro-geometric effects. In addition, the method is recommended by Classification societies for fatigue stress analysis method in

complex ship structures. The weld characteristics and the resulting local nonlinear stress peak are included to $S-N$ curve.

However, parts of structural designs are so complicated both in their geometry and load combinations that the results of rule based modeling approaches can be questioned. The simplified geometry constructed with shell elements and the missing weld have an influence on the stress results. The weld can be modeled for example with shell elements, but offsets still remain. The proper geometry and stiffness representation is achieved with solid models. The lug plates often show fatigue failure in numerical analysis (Lindemark et al. 2009), but based on extensive use of these details in industry, there should not be fatigue failure. The stresses of solid models are closer to experimental results than the ones obtained from shell models. Classification societies do not have detailed guidance on how to perform analysis with solid models. The drawback of solid models is that they are very time-consuming. The detailed stress states including bending and membrane stresses of ship structural detail such as a lug plate connection have not been studied comparing solid and shell element models. Different structural hot spot stress methods including through thickness linearization are not implemented for lug plate connection.

This thesis investigates the suitability of solid element models for fatigue assessment of 3-dimensional ship structural details with complex geometry and stress state. The analyzed 3-dimensional structural detail is the lug plate connection located on the bottom shell of FPSO. The stress state at the lug plate is in special interest. Solid model is used to study the stress as it can better describe the real geometry. Fatigue assessment is done with the structural hot spot stress method and component stochastic spectral method. The structural hot spot stress method is chosen because it is very convenient for engineering design and recommended by classification societies. Results of shell and solid models are compared to see if there is benefit of using solid element modeling in case of lug plate connection. The differences in responses as well as in computational time are discussed.

1.3 Limitations

This thesis is limited to study realistic FPSO conversion project in which the fatigue problems occurred only by the numerical analysis. No real fatigue cracks were found even though the calculation showed them. The thesis does not take stand on the design of structure focusing only the response of different modeling techniques. The 3-dimensional

structural detail is limited to lug plate connection and only the part where offset occurs is studied.

The main focus is on the stress response of different modeling techniques including shell and solid FE models. The solid models are limited to hex meshed models, because they are recommended by classification societies. The fatigue stresses are limited to structural hot spot method even though other methods are discussed in literature review. Hot spot stresses are presented by principal stresses and the angle of principal stress is not taken into account.

For fatigue damage calculation the loads play major part in calculation process. Thus, the spectral methods are introduced and discussed. The fatigue loads are considered as input value in this thesis and thus, this part is not studied in detail.

1.4 Methodology

Ships are large and have complex structures and loads. Therefore, ship structural strength is ensured with FEA. The fatigue is very local phenomenon and thus, very dense meshes are required to capture stress and deformation responses correctly. Large models with dense mesh are not possible to solve in reasonable time in engineering practices. Thus, the sub-models are necessary. In this thesis, sub-models are used to calculate stress response of lug plate for fatigue analysis. Two kinds of sub-models are used: shell and solid models. Shell models are recommended by classification societies. Solid models are rarely used in the practical ship design, but examples can be found in research.

Structural hot spot stress methods can be divided into two (e.g. Fricke 2015): surface extrapolation and through-thickness linearization. Extrapolation method is recommended by classification societies and thickness linearization method is more commonly used in scientific practices. Extrapolation method is commonly used in shell models. For solid models, the extrapolation method is more seen in research purposes. Through-thickness method requires several element layers in thickness direction to produce reliable stress response. Extrapolation method is more closely related to fatigue test, because the stresses on the test are determined from surface of structure in front of the weld toe.

From through-thickness linearization the bending, membrane and non-linear stress peak can be derived for solid models. For shell models, the bending and membrane stresses can be derived from top and bottom surface stresses. From membrane and bending

stresses, the structural hot spot stress can be calculated. Membrane and bending stress also describes the local behavior of the structure near the weld toe. In the bending dominant behavior, the bending stress can be reduced in certain details (DNV GL 2015). Bending reduction is studied with extrapolation method and through thickness method.

Environmental loads that ship encounters during design life can only be described statistically by means of probabilistic methods. Thus, in fatigue assessment the spectral method is used in load determination. Idea behind this method is to describe the true environmental loads, which vessel is intended to encounter with an energy spectrum. Spectrums are presented in frequency domain. For this reason, the loads can be superimposed due to linear behavior. The spectral methods can be divided to full spectral method and component stochastic method (DNV GL 2015). The component stochastic method is used in this thesis because it is more suitable in design process.

2 State of the art

2.1 Wöhler diagram

Wöhler was the first who understood that fatigue damage depends on the amplitude of cyclic stress (Milella 2013, p.2). His discovery was named as a Wöhler's law. Based on the results of his work, logarithmic $S-N$ curves, also known as Wöhler diagram, were published initially by American Basquin (Milella 2013, p.2). The $S-N$ curves are the basis of the modern engineering tool for fatigue analysis.

The $S-N$ curve describes the relation between the cyclic stress range and the load cycles to failure. According to the International Ship and Offshore Structures Congress (2009), the diagram can be divided into three different regime: low-cycle (LC), high-cycle (HC) and ultra-high-cycle (UHC). For the given regimes the fatigue damage occurs below 10^4 , between 10^4 and 10^7 and over 10^7 load cycles, respectively. Low-cycle fatigue damage can evolve for example in case of ship loading and off-loading (Horn et al. 2009, Lotsberg 2007). High cycle fatigue damage accumulates from environmental forces in case of ships. In offshore structures, significant fatigue damages have occurred in ultra-high-cycle regime (Det Norske Veritas 2011).

The basis of different $S-N$ curves is small-scale fatigue tests (e.g. Fricke 2015). From measured data scatter, design curve is fitted with desired survival probability. The curve is described with equation (1)

$$\log N = \log A - m \log s, \quad (1)$$

where N is the number of cycles to failure at stress range s , A is fatigue constant and m is the slope of fatigue curve. Initially it was assumed that $S-N$ curve terminates at fatigue limit (knee point), below which failure will not occur. The knee point was assumed to be at 10^7 load cycles (e.g. Hobbacher 2008). More recent the two-slope $S-N$ curves are implemented and the knee point describes the point, where the slope of $S-N$ curve changes. The design curves describe the total fatigue life to final fracture, without distinguishing between the crack initiation and propagation phase. This is a drawback since it is still unclear how well a single stress component can describe the crack initiation and propagation phases at certain location (Fricke 2015).

2.1.1 Adaptions of S-N curve based on fatigue analysis

The International Institute of Welding (IIW) (Hobbacher 2008) has published standardized curves for different weld types and welding arrangements. Curves are denoted with fatigue design class, FAT, which means allowable nominal stress range at two million load cycles with the survival probability of 97,7% (e.g. Radaj et al. 2009). IIW (Hobbacher 2008) have separated curves for aluminum and steel materials. For aluminum materials the FAT classes are lower in general. The ultra-high-cycle regime is taken into account with bilinear curve, which have slope of 22 in UHC regime and slope of 3 in HC regime. In general steel and aluminum structures related to normal stress have slope of 3. Steel structure curves related to normal stress are constant after the knee point at 10^7 cycles. For aluminum structures on the basis of normal stress the curve is bilinear. For the curves related to shear stress the slope is 5 and knee point is at 10^8 load cycles. Also thickness effect of base material can be taken into account by multiplying FAT class with thickness factor.

There are other design curves available from different design codes such as Eurocode 3 (European Committee For Standardization 1992) for mainly civil engineering design. Ship and offshore classification societies have also their own design curves for example DNV rules for offshore structures (Det Norske Veritas 2011) and DNV rules for ship design (Det Norske Veritas 2010). For marine structures design curves are adjusted for different environments that the structures encounter:

- In air
- Corrosion protection
- Free corrosion

These curves have different fatigue constant and knee point. Also for example in DNV (2011) air and corrosion protection design curves are bilinear, but free corrosion curves are linear. There are also equalities between different curves, for example DNV air curves correspond IIW design curves (Lotsberg 2007).

The *S-N* curve is also characterized based on the stress:

- Nominal stress
- Structural hot spot stress
- Notch stress

For nominal stress there are plenty of different curves for different structure and weld arrangements. According to Niemi et. al (2006), it is recommended to use two design curves for steel structures (FAT100 and FAT90) and two for aluminum structures (FAT40 and FAT36) in structural hot spot method. Lower FAT classes are used in joints with load carrying fillet weld and longitudinal attachments at plate edges (attachment length is more than 100 mm). For notch stress approach, there is only one design curve for steel (FAT225) and aluminum (FAT71) (Radaj et al. 2009).

2.2 Fatigue stress analysis

2.2.1 Nominal stress approach

The nominal stress approach is global in contrast to other S-N based methods. This means that all the macro-geometrical discontinuities and local weld profile are included to relevant design curve and therefore the stress disregards the local stress increase of structural discontinuity and weld geometry (Fricke 2015, Goyal 2015), as shown in Figure 2. It is assumed that some quality factors such as misalignment and residual stresses are indirectly taken into account in *S-N* curves to a certain extent (Fricke 2015, Hobbacher 2008). In IIW guidelines (Hobbacher 2008) the thickness effect should be considered in case of nominal and structural stress approaches.

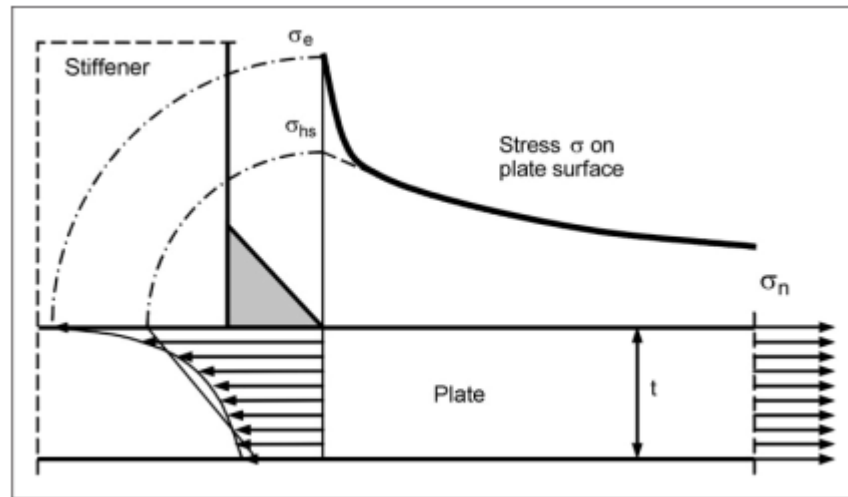


Figure 2. True stress distribution in weld toe region and definition of nominal (σ_n) and local stresses: structural hot spot stress (σ_{hs}) and notch stress (σ_e) (Fricke 2015)

The nominal stress approach is the easiest and most frequently used method to predict fatigue life. Only the nominal stress needs to be determined either by means of linear-elastic theory e.g. beam theory or finite element analysis (FEA). In case of complex

geometry, the determination of nominal stress is difficult and FEA is then the only method to determine stresses. The problem lies in fact; there is no guidance for designer how to calculate the nominal stress using FEA (Goyal 2015).

2.2.2 Structural hot spot stress approach

The structural hot spot stress approach is also known with names of a geometrical stress, structural stress and hot spot stress. The official name is structural hot spot stress according to IIW (Hobbacher 2008) in order to avoid confusion created by the different terms used before. The roots of structural hot spot stress are from offshore industry. The first concepts were developed for tubular joints. According to Fricke and Kahl (2005), in 1960s Peterson, Manson and Haibach tried to correlate the fatigue strength with local stresses. Haibach related a local stress or strain to the fatigue strength at certain distance from weld, for example $1\text{--}2\text{ mm}$. In 1970s method was further developed and the stress read-out points from the weld were dependent on the plate or shell thickness. From these read-out points a fictional structural hot spot is extrapolated (e.g. Fricke 2003). This ideology is still the basis of structural hot spot stress approach.

The structural hot spot stress can be derived either by extrapolating surface stresses or through thickness linearization of plate or shell at the weld toe. This was demonstrated by Radaj (1990). He also proved that a fictitious structural hot spot stress is a sum of membrane and bending stress at the weld toe. Later Fricke and Petershagen derived a generalized approach for complex plate structures using Radaj's effective notch stress approach (Fricke 2003, Fricke and Kahl 2005). Detailed recommendations concerning stress determination were created by several researchers including Niemi and Fricke in 1990s. Niemi et al. (2006) have published comprehensive guidance of hot spot approach and these recommendations have also been updated to IIW guideline.

Fricke et al. (2003) have concluded three different types of hot spot position for plated structures (Figure 3):

- a) weld toe on the plate surface at the end of an attachment
- b) weld toe at the plate edge at the end of an attachment
- c) weld toe along the weld of an attachment

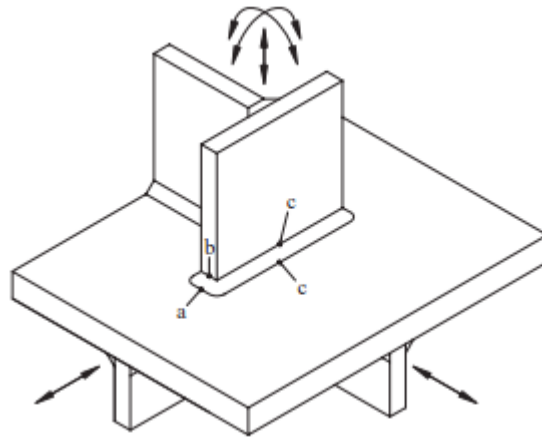


Figure 3. Different hot spot positions.

IIW (Hobbacher 2008) recommends for type a) and c) welds linear extrapolation from points $0.4t$ and $1.0t$ away from hot spot. Stresses are evaluated from nodal points. Several ship classification societies e.g. DNV (2010, 2011) suggest to determine stresses from $0.5t$ and $1.5t$ away from hot spot. An element size equals plate thickness (t). For type b) it is recommended (Niemi et al. 2006) to evaluate stresses from 4 mm , 8 mm and 12 mm from the hot spot. Hot spot stress is achieved by quadratic extrapolation.

In round robin analysis Fricke (2002) studied the effect of modeling and mesh sensitivity to the structural hot spot stress. He found that structural hot spot stress results vary a lot depending on element type, mesh size and even FEA software used. The expected scatter of stress results can be even $\pm 10\%$. The effect of different model types was also studied in (Fricke and Kahl 2005). From the results it can be concluded that both shell and solid models are conservative compared to experimental fatigue test. Especially the selected model of the weld in shell element model affected the results. In 2009 ISSC (Horn et al. 2009) studied different structural hot spot derivation techniques of web stiffened cruciform connections. The presented methods are:

- Classical $0.5t/1.5t$ linear extrapolation.
- Lotsberg's method: shifted stress read-out points depending on plate thickness and weld leg length. Hot spot stress is acquired with correction factor, which depends on bevel angle.
- Osawa's method: read-out points shifted with half of joining plate thickness.
- IACS CSR-B: Classical $0.5t/1.5t$ extrapolation. Hot spot stress corrected with factor depending on bevel angle.

The results show that classical hot spot derivation tends to overestimate the stress. Lotsberg's and Osawa's methods give results in the same range and the corrected classical method is prone to underestimate the stresses. Target hot spot stress was derived with solid model.

For solid modeling Fricke and Kahl (2005) recommends using three or more elements in thickness direction. Reason for this is that the stress singularity created by notch affects linearized structural stress considerably. Lotsberg (2006) agree with Fricke in case of 8-node tetra elements, but in case of isoparametric 20-node elements, the single element in through thickness direction can capture steep stress gradients. In case of complex structures, ISSC committee (Horn et al. 2009) recommends comparing the accuracy of shell models to solid models. True benefits of solid modeling are found in longitudinal connections in the dissertation of Wang (2008) and in Lotsberg's (2005) full-scale test report. In both studies stresses obtained from solid models agree better with experimental data.

There are also other options to determine structural hot spot stress. Dong (2001) has proposed a method, which is a further development of Radaj's through thickness stress distribution method. He evaluates structural stress at weld toe from finite element method by using the principles of elementary structural mechanics. The stress gradient along the anticipated crack path is taken into account by using fracture mechanics. Dong claims that method is mesh insensitive, but Fricke et al. (2003) and Poutiainen et al. (2004) showed mesh sensitivity in case of solid element models.

In contrast to nominal stress, the structural hot spot stress contains macro geometric effects such as the shape and size of welds, when weld is modeled (Goyal 2015). Also stress increase affected by structural geometry is included, but the stress peak caused by the weld toe's sharp notch is excluded (e.g. Fricke 2015), as shown in Figure 2. The structural hot spot stress method is only valid in case of weld toe fatigue failures and weld root failures must be considered with other methods, such as notch stress approach.

2.2.3 Notch stress approach

The notch stress approach is based on calculating the stress peak caused by sharp notches (Figure 2) taking into account different microstructural support approaches. The microstructural support effect approaches can be divided into four methods (Fricke et al. 2003):

- Stress gradient
- Stress averaging
- Critical distance
- Highly stressed volume

Radaj (1990) proposed that the local stress peak can be evaluated directly without requiring stress concentration factor (SCF) or fatigue notch factor. The stress peak can be calculated with fictitious rounding at sharp notch and approach is based on Neuber's stress averaging hypothesis. For fictitious rounding Radaj proposed 1 mm for steel structures with thickness at least of 5 mm by assuming von Mises strength condition. For thinner structures it is recommend to use fictitious rounding of 0.05 mm (e.g. Sonsino et al. 2012). The linear-elastic theory is adopted in stress evaluation and the local principal or von Mises stresses are compared to allowable value. This method is called effective notch stress approach and has been adapted to IIW guidelines (Hobbacher 2008). The effective notch stress approach is applied in many state of art studies (e.g. Sonsino et al. 2012, Fricke et al. 2012, Fricke and Paetzold 2010, Tran Nguyen et al. 2012) in shipbuilding and offshore industries.

Compared to nominal stress and structural hot spot stress approaches the effective notch stress approach takes into account macro and micro geometrical features such as weld leg length, weld toe angle and shape of weld (Goyal 2015). Also the thickness effect is included in stress (Fricke 2015).

Effective notch stress calculation requires very detailed high density finite element models. The IIW (Hobbacher 2008) recommends using elements sizes of $1/6$ and $1/4$ of radius for linear elements and higher order elements, respectively. Thus the calculation time increases dramatically compared to structural hot spot stress method. The amount of elements grows in large structures, so the implementation in large structure models requires sub-modeling technique.

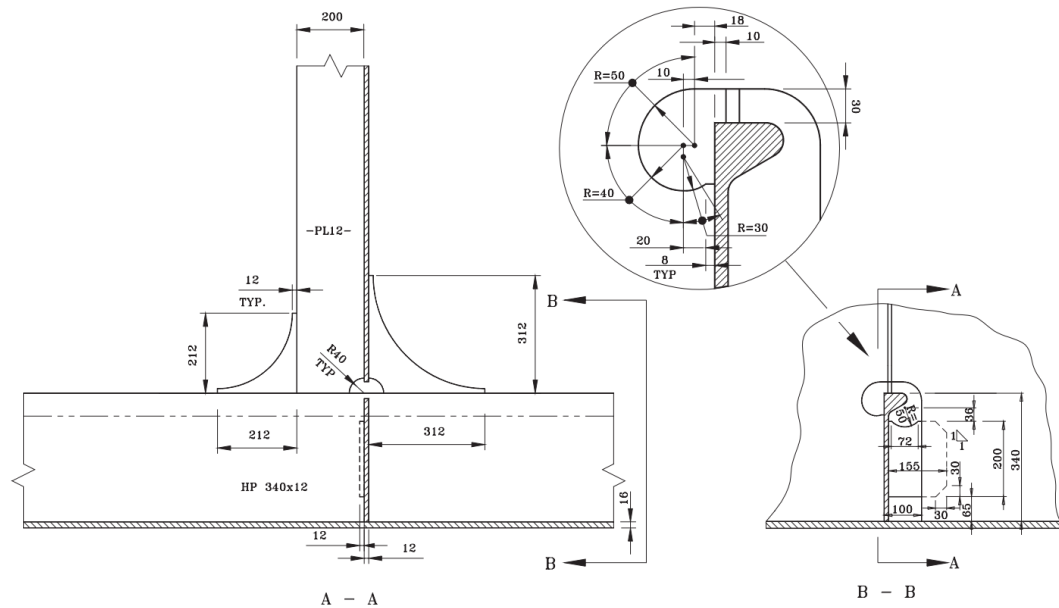
2.3 Effect of modeled weld

In general, the stress state in weld toe is multi-axial in nature, but in most cases the stress component in normal direction to weld toe is predominant (Radaj et al. 2009, Chattopadhyay 2011). The shell elements reduce stress components to three: two-in-plane and one non-zero shear components. Model created with shell elements also simplifies the geometry to mid-planes. This can cause problem when the structural offsets should be modeled and additional stress singularities are created. The shell stresses are highly dependent on the local stiffness of the joint in the weld toe region and therefore it is crucial how the local stiffness is accounted for in the shell element model (Chattopadhyay 2011). The welds should be modeled when the weld is affected by high local bending due to offset between plates or due to small free plate length between adjacent welds e.g. lug plates (Lotsberg 2006). The welds should also be modeled when it is difficult to distinguish between the notch itself and geometrical irregularities in the stress concentration (Aygül 2012). Such a case is when the hot spot is near openings. There are mainly three different approaches to model stiffness of weld: rigid links, bar elements and shell elements (Aygül 2012). DNV (2010) recommends modeling welds with shell elements, which thickness is two times the adjacent plate thickness. Same weld modeling technique is adopted by International Association of Classification Societies (IACS).

2.4 The determination of three dimensional structure

Three-dimensional ship structural details are details, which cannot be properly modeled with shell elements. The key in determination of three-dimensional ship structural details is that the detail is mainly affected by high local bending due to shear. The modeling of details is hard with shell elements because of the presence of weld and the local stiffness affects the results. Also in case of lug plate, there is eccentricity created by offsets. The 8-node plate element takes the local bending into account better (Hobbacher 2008), but it does not remove the effect of weld. Chattopadhaya (2011) has developed special meshing technique for shell element models, which includes the weld. Method suffers from very time-consuming modeling phase. The more convenient way to model the problem is using solid elements, where the geometry and the weld stiffness are accounted properly. The examples of 3 dimensional structural details are (Figure 4):

- Longitudinal cut-out details with lug plate
- Scallop corners
- Bracket tips at bracket side



Norske Veritas 2010). In the simplified rule based method the stresses are based on rule loads, which can be either analytically derived or from FEM. The long-term stresses are determined with two parameters in Weibull distribution. The Weibull distribution is defined by a shape parameter and a reference stress at an appropriate probability level (Horn et al. 2009). The shape parameter depends on the type of ship, sailing route and location of the structural detail (Hughes and Paik 2010 p. 17-13).

2.5.1 Spectral analysis

In spectral analysis, the stresses are determined with a ship direct linear motions and load analysis. Instead of calculating ship motions and responses in time domain, these are calculated in frequency domain. Frequency domain provides more straightforward procedure and it is more time-effective compared to time domain solution. In addition, the principle of superposition is applicable. (Karadeniz 2013 pp.105-106)

The response spectrum is achieved by multiplying wave spectrum and response amplitude operator (RAO), which is an absolute value of a squared transfer function (Matusiak 2013 p.103). A sea state is a combination of multiple waves with different frequencies, amplitudes, phases and directions and it is described by its energy spectrum, i.e. the wave spectrum (Hughes and Paik 2010 p.17-10). There are many different wave spectra available for different sea areas. For example, ISSC spectrum is suitable for describing the developed ocean waves and Jonswap spectrum is better suited for sheltered sea areas with limited fetch and for raising storm (Matusiak 2013 p. 75). Transfer functions describe ship's motions and load effects in the sea. It depends on ship's heading and speed and can be determined from linear approximation of strip theories or panel methods or even experimentally by conducting model tests in regular waves (Matusiak 2013 p.102). Transfer function has to be calculated for different operational conditions of a ship. In general spectral fatigue analysis procedure takes into account the different operational and environment conditions by weighting the different conditions by their occurrence probabilities (Kukkanen 1996 p.28).

Spectral methods can be divided to component stochastic analysis and full stochastic analysis. In full stochastic analysis hydrodynamic and structural analysis are automatically linked. All the hydrodynamic loads including panel pressures, internal tank pressures and inertia forces due to rigid body accelerations are transferred to finite element model. In addition, phase information of loads is automatically included in the

analysis. The finite element model is either full global or cargo hold model. Local calculations are done in sub-models driven by global model boundary displacements. In sub-models, the local internal and external pressures and inertia loads are transferred from the wave load analysis. In order to ensure correct results, the mass and mass distribution of hydrodynamic model and global model must be similar. (Det Norske Veritas 2010, 2012)

In component stochastic procedure, load transfer functions are calculated separately for each load component in hydrodynamic analysis. Stress responses per unit load (Stress response factor) for each load component are calculated separately in finite element model. Phasing between different load components is taken into account in load transfer functions. Thus, the load transfer functions can be summed up. In some cases, the separation of different load effects is not easy and duplication may occur. Also fictitious global bending moments can occur when local loads are applied. One major advantage in component stochastic method is that a nonlinear effect, such as the pressure reduction at waterline is relatively easy to take into account. (Det Norske Veritas 2010, 2012)

In full stochastic method, the structural model always requires correct mass distribution. In other words, the hydrodynamic model and the structural model must be balanced. Thus, the full stochastic method requires all the structural information and it is more proper for verification of final design. The load component stochastic model does not require weight-balanced model. It can be created in an early design phase and gradually updated during design process. This requires updated RAOs during the design process. This is a major advantage compared to full stochastic procedure. In addition, smaller models can be used. Also it allows studying the effects of each load component and most significant loads can be identified. One can say that load component method is more design-oriented tool.

2.5.2 Damage model

The most common and one of the simplest damage models is known as the Palmgren-Miner approach. It is assumed that fatigue damage accumulates linearly and the order of occurred loads in time does not matter. The damage is calculated as a ratio of number of cycles n_i and number of cycles to failure N_i under constant stress range s_i . Because linear damage accumulation for different stress ranges over life time is assumed, the total damage is then simply the sum over all constant stress blocks, as shown in equation (2).

$$D = \sum_{i=1}^k \frac{n_i}{N_i} \leq 1 \quad (2)$$

The total damage ratio D is expected to be less than unity in order the structure to survive (Hughes and Paik 2010 pp. 17-39-17-40). In general, design maximum allowable damage ratio is often manipulated with safety factors yielding lower acceptable damage ratios. IIW (Hobbacher 2008) recommends for spectra with high mean stress fluctuations the maximum damage ratio of 0.5 or even 0.2. For probabilistic analysis, Karadeniz (2013) recommends determining damage ratio as random with mean value of unity.

Damage calculations in spectral analysis require information about the long-term stress distribution. The distribution is described with probability functions. The Weibull probability density function has been found to fit best to represent long term stress distribution (Hughes and Paik 2010). Alternatively, the long-term stress distribution can be defined as a series of short-term distributions based on wave scatter diagram. Short-term stress distributions are described by Rayleigh probability function (Hughes and Paik 2010). In simplified approach of damage calculations, each long-term histogram is converted into a step-curve, see Figure 5. Hughes and Paik (2010) recommend using at least 40 steps of equal length and DNV (2011) 20 steps. Then the damage ratio is calculated for each step and summed. More common and modern way to calculate damage is to use wave scatter diagram and Rayleigh distribution. The damage is calculated for each sea state in scatter diagram and summed.

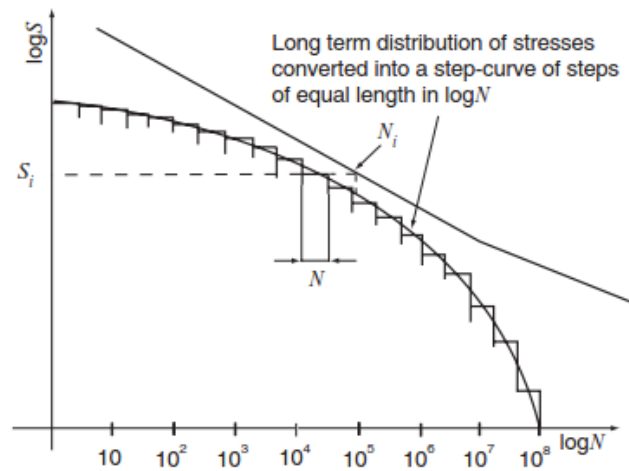


Figure 5. Transformation of long-term stress distribution to step-curve (Hughes, Paik 2010).

3 Methods

3.1 Sub-modeling

Due to complex structural topology of the large ships, the FE method is the only way to determine the structural response in required accuracy. The response of ship structures is evaluated in three different stress levels (Lewis 1988):

- Primary response to evaluate global response of vessel
- Secondary response to evaluate e.g. double bottom structure
- Tertiary response to evaluate e.g. stiffened plates

In addition to these, the small details e.g. lug plates are evaluated at local level. The required response level defines the used mesh density. For example, for the primary response the mesh size is selected by web frame and frame spacing and for structural hot spot fatigue analysis by plate thickness. A sub-model mesh density must be fine enough to capture the required stress response. Global model mesh size is too coarse to capture the non-linear stress peaks and denser mesh in global model is not reasonable because the calculation time increases rapidly. Because of this demand of dense mesh size for local analysis the sub-models are needed in order to solve FE-models in reasonable time.

Global models are used to capture overall behavior of ship structure. Typically for bulkers, tankers and FPSO's the cargo hold model is enough to capture force flows in structures and can be used for screening critical locations. Usually three or more cargo holds are included in the model depending on the studied area and size of the ship. From global model the boundary conditions are applied to separate local sub-models. Industry standard is to use nodal displacement as boundary conditions for sub-models (DNV GL 2015). The best accuracy is achieved when nodes from global model to sub model coincide, but nodal displacements can also be interpolated to sub-model. It should be noted that separate sub-model should have equal stiffness to the respective part of the overall model (Prayer and Fricke 1994). Stiffness changes between models change the force flow at model boundaries. Adequate information change between models can be checked against force flow. This means that the information goes from global model to sub-models and if the structural details change remarkably in the sub-model, the global model should be updated as well. This can be avoided with super-element technique where information between models goes two ways (Cook 2001). Third way is to use direct mesh refinement in the studied area (Prayer and Fricke 1994). This method is not possible in global model in fatigue analysis because the amount of details is large. But it is very

useful method inside sub-models and gives results with good accuracy. Also the amount of the separate sub models decreases.

The amount of local details that need to be analyzed is high in ship structures. The size of the sub-models depends on the analyzed structure and the amount of the details that can be included in terms of computational time. The results near the boundary of the sub-model are affected by forced nodal displacements. The St. Venant's Principle applies and the boundary of the model should be far enough from the analyzed detail.

The shell-solid sub model boundary is trickier because in addition to the displacements also the rotations of the shell model need to be transferred to solid model. This can be done manually, but it requires a lot of time in fatigue analysis. To avoid this extra work, the use of shell-solid coupling simplifies the problem because rotations are transferred straight away between models. The common methods for coupling of solid and shell models are multipoint constraint (MPC) equations, rigid link connection or perpendicular shell coupling method (PSCM) (Osawa et al. 2007). The MPC causes only a little or no stress disturbance in boundary of models, but evaluation of coupling equation can be so troublesome that in design it becomes impractical. Rigid links can cause a lot stress disturbance in the vicinity of the model's boundary. In PSCM a fictitious perpendicular shell plate is attached on boundary of shell and solid model. The PSCM method gives good results but its' drawback is that elements between boundaries need to be equally sized. The commercial FEA programs such as FEMAP have introduced automated tools to couple shell and solid models for engineering purposes. In FEMAP this is called Glued connection. Its' benefits are that meshes do not need be equal on the boundary of shell and solid models (Siemens 2015). Although accuracy will decrease when difference between mesh sizes increases notably. Principle drawing of coupling of shell elements and solid elements via glued connection is shown in Figure 6.

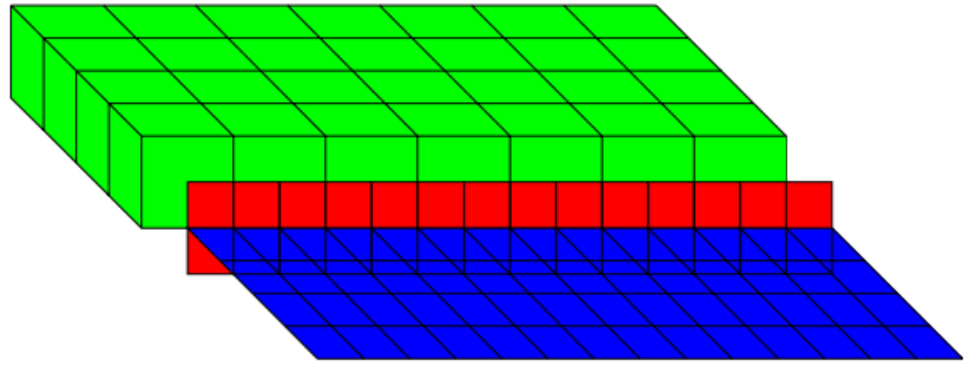


Figure 6 Shell-solid coupling by glued element. The blue color represents shell elements, red color represents glue elements and green color represents solid elements.

Generally, the denser mesh is selected as master (source) region and sparse mesh as slave (target) region. The Nastran solver creates glue elements, on precision of source region. These elements correctly transfer displacements and loads on connection region (Siemens 2015). On the shell-solid coupling the shell edge shall be selected to source region regardless of the mesh density. Then the accuracy of glued connection can be improved with refinement parameter, which projects the denser mesh grid to source region and creates glued elements based on the denser mesh (Siemens 2015). In this way, the better distribution of glued elements and result is achieved.

3.2 Solid modeling

Solid FE-models consist of three-dimensional elements. Isoparametric solid elements have three degrees of freedom (DOF) per node and six strain and stress components. Solid elements can be divided to linear and parabolic elements based on the shape functions. Elements can also be categorized by geometric shape of the element. The common element types are hexahedron (hex, brick), pentahedron (wedge) and tetrahedron (tetra). From these the tetra is the easiest to model and the most commercial FE modeling software have good automated tools in meshing. Brick meshing requires the most geometric preparation of the model for creating the mesh. In hex modeling the difference between FEM programs start to differ. Finite element software HyperMesh has been found good in hex meshing and was used for mesh preparation in this thesis.

In hex modeling the geometry must be divided to parts whose opposite surfaces are coincident. In other words, the geometry is divided to extruded parts. Therefore, complex

models are very time consuming to mesh. HyperMesh has specialized tools to divide the geometry and it recognizes and can change information of mesh sizes on the boundaries of extruded geometry parts. Generally meshing is started from smallest detail, which requires the densest mesh and eventually meshed towards the boundaries of the model. The smallest detail defines the mesh size of the surrounding structures.

In case of simple T-cross joint the mesh creation is straightforward and the weld defines the smallest element size. Because of the shape of T-joint the elements can be in one layer. In case of lug plate connection, the weld also defines the element size. But because the weld goes around the lug plate and the lug plate is connected to webframe, elements cannot be arranged to one layer. The weld divides the webframe and lug plate to two layers and hence the minimum amount of element layers is two in lug plate connection. The Figure 7 will clarify this.

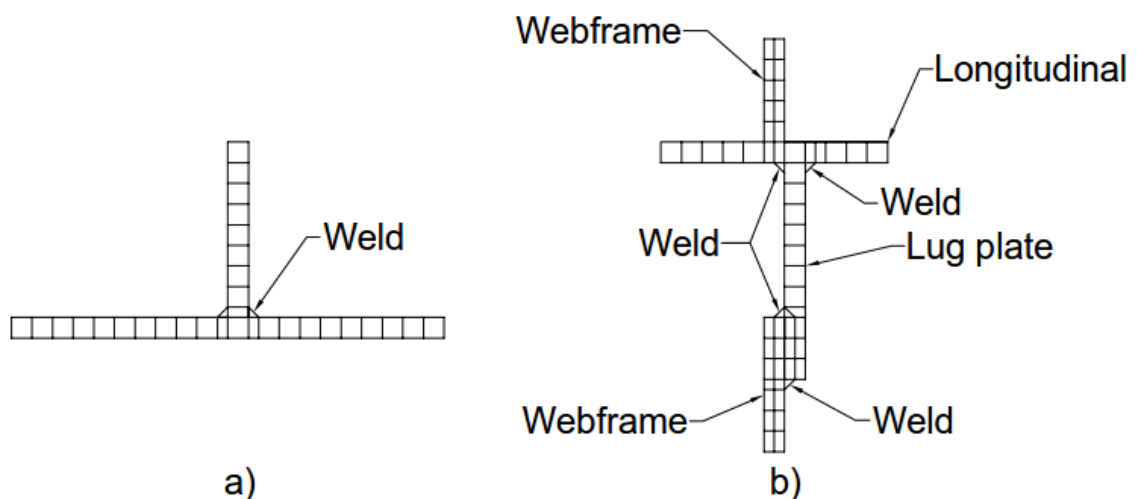


Figure 7. Solid meshing principles of simple T-joint (a) and lug plate connection (b).

The mid-planes of solid elements should be coincident with the mid-planes of shell elements. In practice, shell models are constructed to molded lines of ship structures in ship design. This means when the geometry is modeled by actual 3-dimensional structure to mid-planes of the shell elements the dimensions differ between shell and solid models.

The following simplifications are made in construction of solid model:

- the lug plate dimensions are kept the same in both models meaning that opening size is increased in solid model
- the bracket on top of longitudinal is shifted upwards by increased height of stiffener in solid model.

In addition, the net scantlings are applied. This means that corrosion allowances are deducted as per ABS (2014) rules. This affects to lug plate and webframe connection increasing the offset between structural parts. In order to create simple mesh, the physical gap due to corrosion deduction is disregarded and lug plate is modeled with physical connection to webframe.

3.3 Derivation of hot spot stress

3.3.1 Extrapolation procedure

The extrapolation procedure follows $0.5/1.5t$ method, which is recommended by ship classification societies (e.g. Det Norske Veritas 2010). Used mesh size determines available stress read-out-points (ROPs). For $0.5/1.5t$ method it is recommended to use thickness time thickness mesh, when stress can be read on element stresses or nodal points. Then element stresses are on $0.5t$ and $1.5t$ distances from hot spot and straight extrapolation can be conducted. If nodal stresses are used the stress ROPs are at $1t$ and $2t$ distances from hot spot and quadratic polynomial curve can be fitted and stresses extrapolated on curve positions at distances $0.5t$ and $1.5t$. If the mesh size is more arbitrary or more than three read-out-points are used the order of polynomial curve can be increased. This can lead to oscillating curve which does not represent stress gradient at hot spot. Therefore, higher order polynomial curves are not recommended on structural hot spot stress derivation.

When the used mesh size is about thickness time thickness, the nodal points do not lie on the desired extrapolation points. For this reason, the stresses are read from actual nodal distances and quadratic curve is fitted. An example of curve fitting and extrapolation points is shown in Figure 8.

Quadratic fit is recommended by Niemi et al. (2006) and DNV (2011) when the stress ROPs are not located on exact locations and straight extrapolation is not possible. Det Norske Veritas has limited element size from $t \times t$ to $2t \times 2t$, but Niemi also proposes smaller elements than $t \times t$.

American Bureau of Shipping (2014) requires that hot spot stress has to be extrapolated to actual weld toe location. In case of shell model, the stresses are read from same points as earlier discussed, but the extrapolation points ($0.5t$ and $1.5t$) are shifted by weld leg

length on quadratic curve fitting. Then linear extrapolation is conducted at weld toe location.

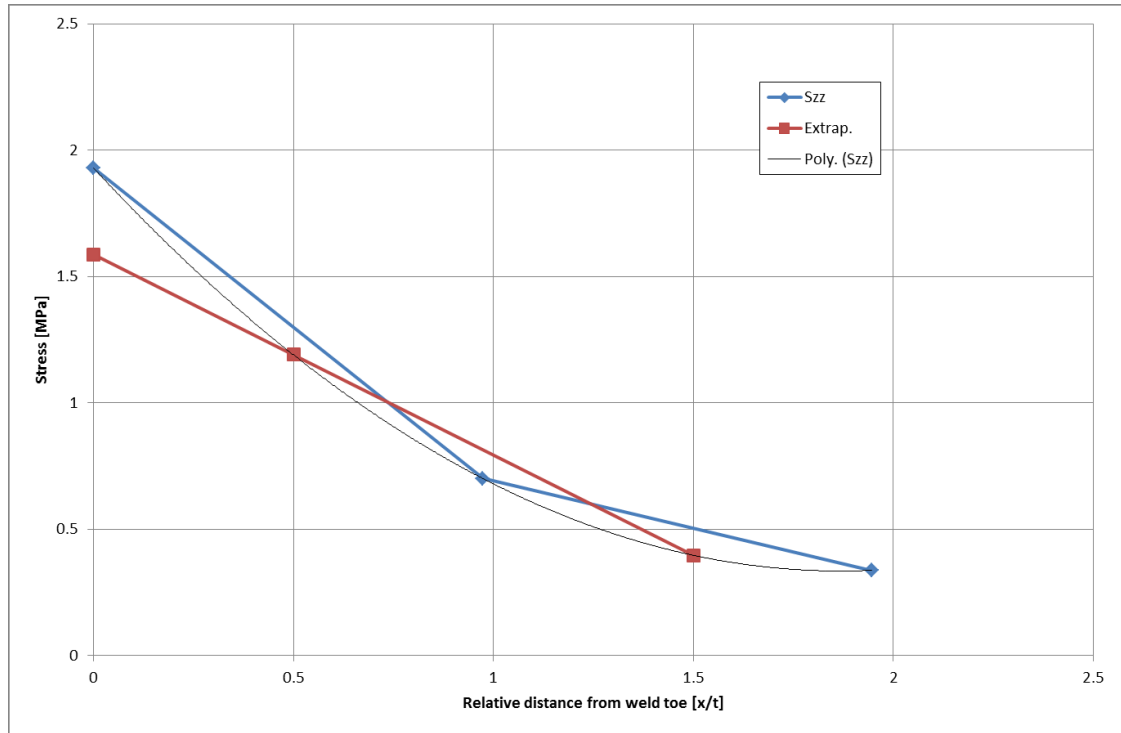


Figure 8. An example of extrapolation procedure and quadratic curve fitting of one stress component. The blue dots are stress results from FEA and thin black line represent quadratic curve fitting. The red curve is extrapolation line.

In this thesis, the maximum non-averaged stresses are read from elements' corner results and averaged between adjacent elements, when the same node is shared by two elements on the extrapolation path. In general, it is recommended to evaluate stresses from surface stress components in $0.5/1.5t$ method. In case of 3-dimensional solid elements some FEM programs can only provide the average element stress not stresses on element sides. Therefore, it is more practical to use nodal stresses, which are generally accepted to be more accurate than element stresses. When the stress ROPs are located at $0.5/1.5t$, the extrapolation is conducted without quadratic curve fitting.

The extrapolation is done to each stress component separately and principal stress is calculated from extrapolated stresses. The structural hot spot stress is taken as the maximum absolute value of the principal stresses. The direction of principal stress is not accounted for. The recommendation is to take principal stress direction into account and disregarding of it may lead to conservative result.

3.3.2 Through thickness linearization and stress field

The stress field for type a hot spot can be decomposed for membrane stress, bending stress and non-linear stress peak (Niemi et al. 2006), Figure 9. Figure 9. Stress components at weld. The structural hot spot stress is the sum of membrane and bending stress. According to IIW (Hobbacher 2008) the membrane stress is average stress calculated through the thickness of plate and constant through thickness. Bending stress is linear and goes through the point O, which is on the neutral axis of the plate. On the same point lies membrane stress value. The slope of the linear stress is chosen so that non-linear stress is in equilibrium with linear stress. The non-linear stress peak is then the remaining part of the stress field.

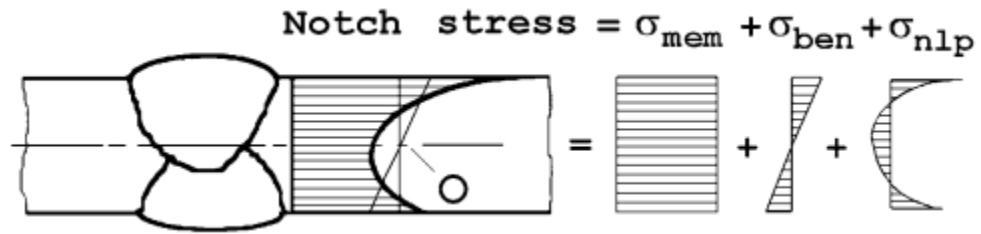


Figure 9. Stress components at weld. Notch stress is sum of membrane (σ_{mem}), bending (σ_{ben}) and non-linear stress peak (σ_{nlp}) stresses. (Niemi et al. 2006)

Mathematically the membrane stress σ_{mem} , bending stress σ_{ben} and non-linear stress peak σ_{nlp} are written

$$\sigma_{mem} = \frac{1}{t} \int_0^t \sigma(x) dx \quad (3)$$

$$\sigma_{ben} = \frac{6}{t^2} \int_0^t \sigma(x) \left(\frac{t}{2} - x \right) dx \quad (4)$$

$$\sigma_{nlp}(x) = \sigma(x) - \sigma_{mem} - \left(1 - \frac{2x}{t} \right) \sigma_{ben}. \quad (5)$$

It can be concluded that the structural hot spot stress is then linear stress distribution of stress field at the weld toe. Thus from the non-linear stress distribution the linear stress distribution can be approximated with the least square method. The membrane stress is average of the linear stress distribution and the bending stress is the difference of the linear stress and the membrane stress. Stress linearization is shown in Figure 10. The

through-thickness linearization is done to all stress components and structural hot spot stress is achieved from principal stress.

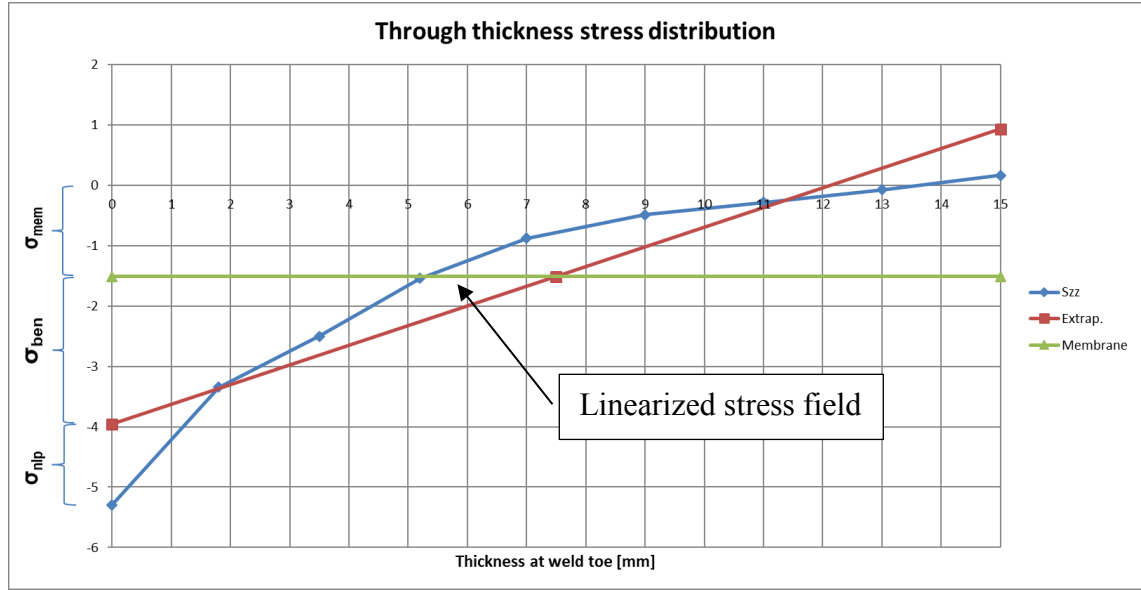


Figure 10. An example of linearized stress field at weld toe. Peak stress consists of non-linear stress (σ_{nlp}), bending stress (σ_{ben}) and membrane stress (σ_{mem}).

For shell element the bending stress and membrane stress are

$$\sigma_{ben} = \frac{\sigma_{top} - \sigma_{bottom}}{2} \quad (6)$$

$$\sigma_{mem} = \frac{\sigma_{top} + \sigma_{bottom}}{2}, \quad (7)$$

where σ_{top} is surface stress component on the top surface and σ_{bottom} is the surface stress component on the bottom surface.

3.3.3 Bending reduction

The bending reduction is based on the fatigue tests performed by Kang et. al (2002). The $S-N$ curves are derived on in-plane loads and therefore do not take into account out-of-plane bending loads. According to Kang et al (2002) the fatigue strength is higher for out-of-plane loads compared to in-plane-loads even if the structural hot spot stress is same. With bending reduced structural hot spot stress, the same $S-N$ curves can be used for details with high bending stress. The reduction is adopted to class rules (e.g. DNV GL 2015), but it is restricted to cases where fatigue crack growth development is displacement controlled rather than load controlled.

There are no clear instructions how the bending stress reduction should be taken into account when calculating the hot spot stress. Generally, the bending reduction means that bending stress component is reduced by 40%, but instruction on how it is done step-by-step is not written. In this work, the bending stress reduction is divided to two approaches: bending reduction of extrapolation method and bending reduction of through thickness linearization method.

In extrapolation method the bending reduction is taken into account at each stress ROPs. First all stress components are linearized through the plate thickness. Bending and membrane stress is derived from linearized stress field as explained in the chapter 3.3.2. Then bending stress is reduced by 40% and summed to membrane stress. Last the stress components are extrapolated as explained in the chapter 3.3.1.

In through thickness method, the bending reduction is taken into account at the weld toe location. From thickness linearized stress, the 40% bending reduction is done to bending stresses of each stress component. The hot spot stress is principal stress calculated from bending reduced stress components.

3.4 Fatigue assessment

Fatigue assessment can be divided to three parts. It consists of load part, structural response part and strength part. The schematic diagram of fatigue assessment used in this thesis is shown in Figure 11. Load part consists of items 1-4, response part items 5-11 and strength part item 13. Load part is not in scope of the thesis and load information is used as input. However, it is shortly introduced as it is essential in fatigue assessment.

In load part, the transfer functions of each load components are determined by hydrodynamic analysis. This is done in AQWA software, which uses 3-D panel theory in load determination. Loads are calculated for different unit waves with different headings for selected loading conditions. In AQWA, linear wave theory is used in determination of wave-induced loads. From AQWA analysis RAOs (load transfer functions) are obtained for accelerations, motions, pressures, moments and forces.

The response part consists of FE model and analysis of it. First the geometry of structures is modeled and then meshed. FE models are divided to global model and separate sub-models. The global model is solved first and the boundary conditions to sub-models are

obtained from it. Used models are described in chapter 4.2. The sub modeling and solid modeling principles are discussed in chapters 3.1 and 3.2, respectively.

For selected ship's loading condition, FEA sub-models are solved by unit loads, which are presented in chapter 4.2.5. Results are then stress responses by unit loads. From these stresses the structural hot spot stress per unit load is evaluated by extrapolation technique. The stress RAO (stress transfer functions) are calculated for each unit wave load RAOs as a function of wave frequency. The stress RAO is the multiply of the hot spot stress and unit wave RAO. The real part and imaginary part are calculated separately. Combined transfer functions are obtained by summing all stress RAOs. The stress spectrum is calculated using the combined transfer function and corresponding wave spectrum.

For fatigue damage calculation the stress spectrum, wave data and S-N curves are needed. For wave data the actual scatter of sea environment of the tanker sailing condition is used. The long-term response is achieved by Rayleigh model (summation of short-term predictions by weighted occurrences) with the Wirsching Light wide band correction as recommend by ABS (2013). The damage is calculated to each sea-state in scatter diagram with ABS' offshore E curve. Cumulated fatigue damage is calculated with Palmgren-Miner rule with design life of 3.15 years, which is based on the data the vessel has encountered.

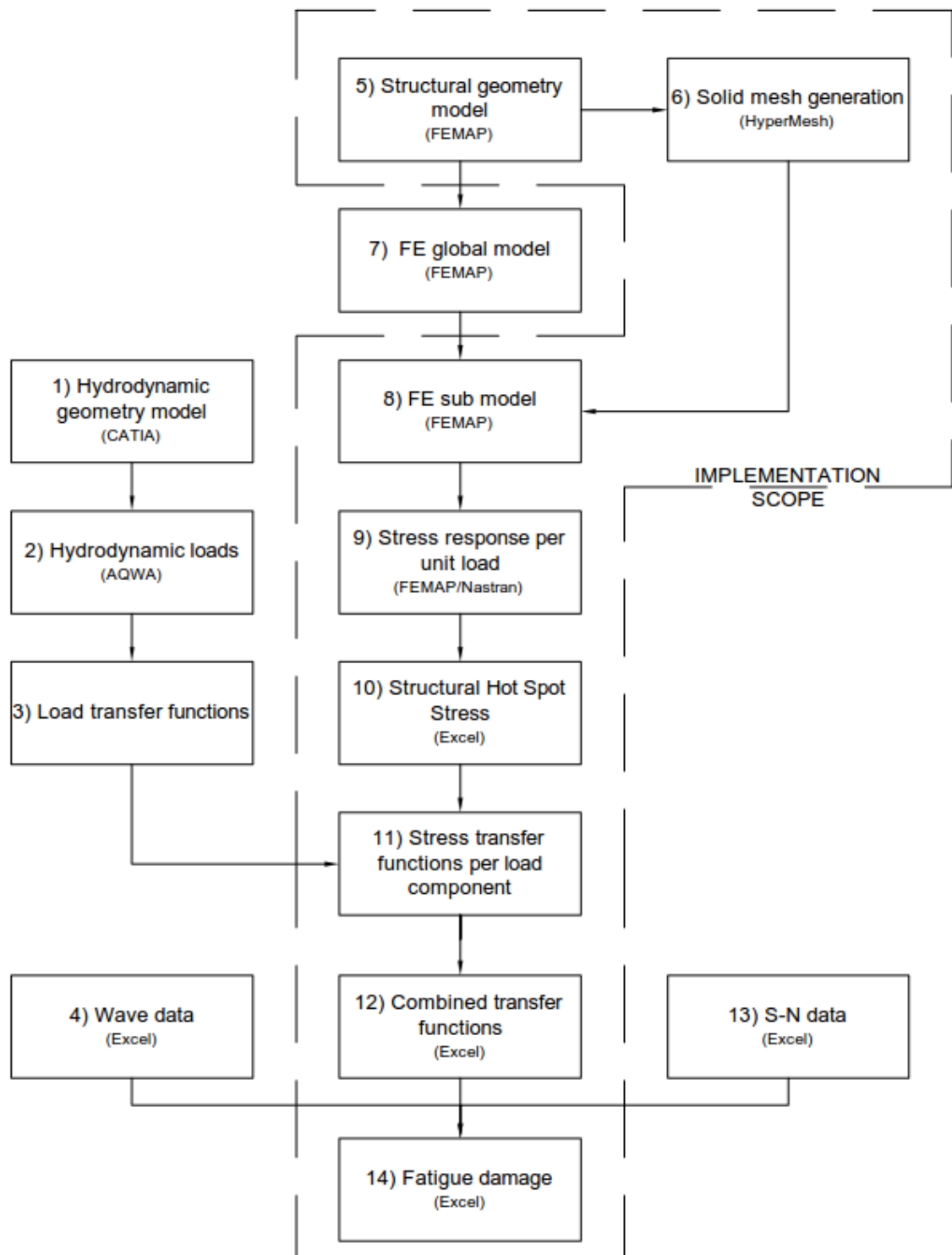


Figure 11. Schematic diagram of fatigue assessment produce.

4 Case description

4.1 General

In an oil industry floating production, storage and offloading ships (FPSOs) are tempting alternative for oil production. Especially in deep water environments FPSOs are generally recognized as the most cost efficient solutions for oil production (Shimamura 2002). The construction and design time cycle of FPSOs are lower compared to the fixed offshore structures. Also change of oil production field is easier due to hull form, which is same type as in ships. Many of the FPSOs have been converted from crude oil tankers. Conversions from a crude oil tanker to a FPSO have shown for owners significant cost and schedule benefits compared to a newbuilding FPSO (Le Cotty and Selhorst 2003).

The FPSO conversions have special design rule requirements. The load histories of tanker phase and future FPSO phase have to be taken into account in fatigue analysis. If tanker phase historic data is not known, the North Atlantic data is used. Otherwise the realistic history is used. For FPSO phase site-specific data is used. In practice this means direct fatigue analysis using spectral based approaches. Direct fatigue stress analysis typically shows higher stress concentration factor (SCF) of details compared SCFs implemented straight from rules. Potential reasons for this can be found in FEA modeling. Shell elements might not be good to represent all geometry details such as weld, longitudinal connection with bracket or offsets. A lug plate is one of the details which has shown in many cases high SCFs compared to rules.

In case study the previously discussed methods are tested on a real FPSO conversion project. The case FPSO conversion is made from tanker, which has been sailing for 20 years. The main particulars of FPSO are presented in Table 1 and profile of the ship is shown in Figure 12.

Table 1. Main dimensions of FPSO.

Quantity	Unit	
Length btw perpendiculars, Lpp	257.00	m
Length waterline, Lwl	260.50	m
Scantling length	252.68	m
Breadth moulded	42.50	m
Depth moulded	22.40	m
Scantling draught	15.50	m
Block coefficient	0.885	-
Transverse spacing	4390	mm

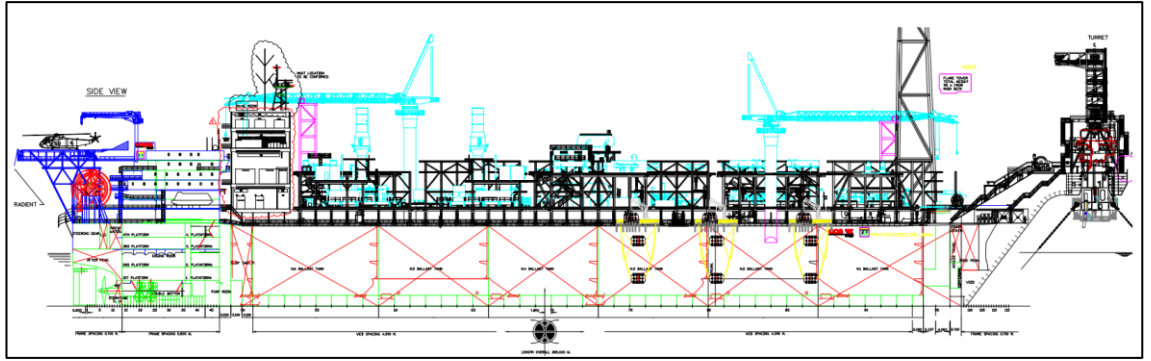


Figure 12. The profile of FPSO

The detail under the study is a lug plate on ship's double bottom. The lug plate locates close to midship. The hot spot stress response of unit pressure loading is compared between shell and solid FE-models. For response analyses selected ship's loading case is full load and used component load is FL8, which is a pressure strip on bottom at the lug plate location. The effect of different solid model approaches on weld corner and effect of gap between lug plate and web frame are tested. In addition, the severity of different load components on damage level is compared using the component stochastic spectral analysis.

4.2 Model description

4.2.1 General

The shell models and geometry of solid models are prepared in FEMAP v11.2 software. The solid mesh is created in HyperMesh v12.0. Nastran is used as solver and post-processing is done in MS Excel.

4.2.2 Model hierarchy

The modeling hierarchy is divided to three levels: global model, semi-sub-models and sub-models, see Figure 13.

The global model contains three cargo holds of the ship from frame #57 to frame #82. The structure is modeled with shell elements except for stiffeners, which are modeled with beam elements. Mesh size is 5 elements between web frames and one element between stiffeners. The model is used for calculating global deformations of the ship hull. Deformations from the global model are applied to semi sub models and sub models.

Semi sub-models are plate models applied for fatigue analysis with thickness sized mesh density at hot spots. The semi sub model extent is from frame #67 to #71, from port side to longitudinal L17 and from bottom to first horizontal girder. All of the structures are modeled with shell elements except for the stiffeners flanges, which are modeled with beam elements. The shell element size is $200 \times 200 \text{ mm}$ far from the lug plate location and gradually decreases to $t \text{ mm}$ at the lug plate location. On free edges of holes and brackets dummy rod elements are inserted according to ABS guidelines in order to reduce fictional stresses. Structures are modeled using net scantlings, which means that corrosion allowances are deducted from as built thicknesses.

Sub-models are solid element models of the lug plate connection. Models are used for fatigue calculations by means of hot spot stress method. Models consist of two parts: shell model and solid models, which are connected to shell model with FEMAP Glue connection. The shell model extent is the same than in semi sub-model, but solid model extension varies depending on the model. The Solid20W models extend from mid span of web frames containing one longitudinal spacing. Upper edge of models is at mid height of double bottom. The mesh size is about $t \text{ mm}$ and $t/2 \text{ mm}$ in thickness direction. The Solid8W models extent 5 times of the lug plate thickness to every direction from the hot spots. The mesh size of the Solid8W models is $t/8 \text{ mm}$ in every direction.

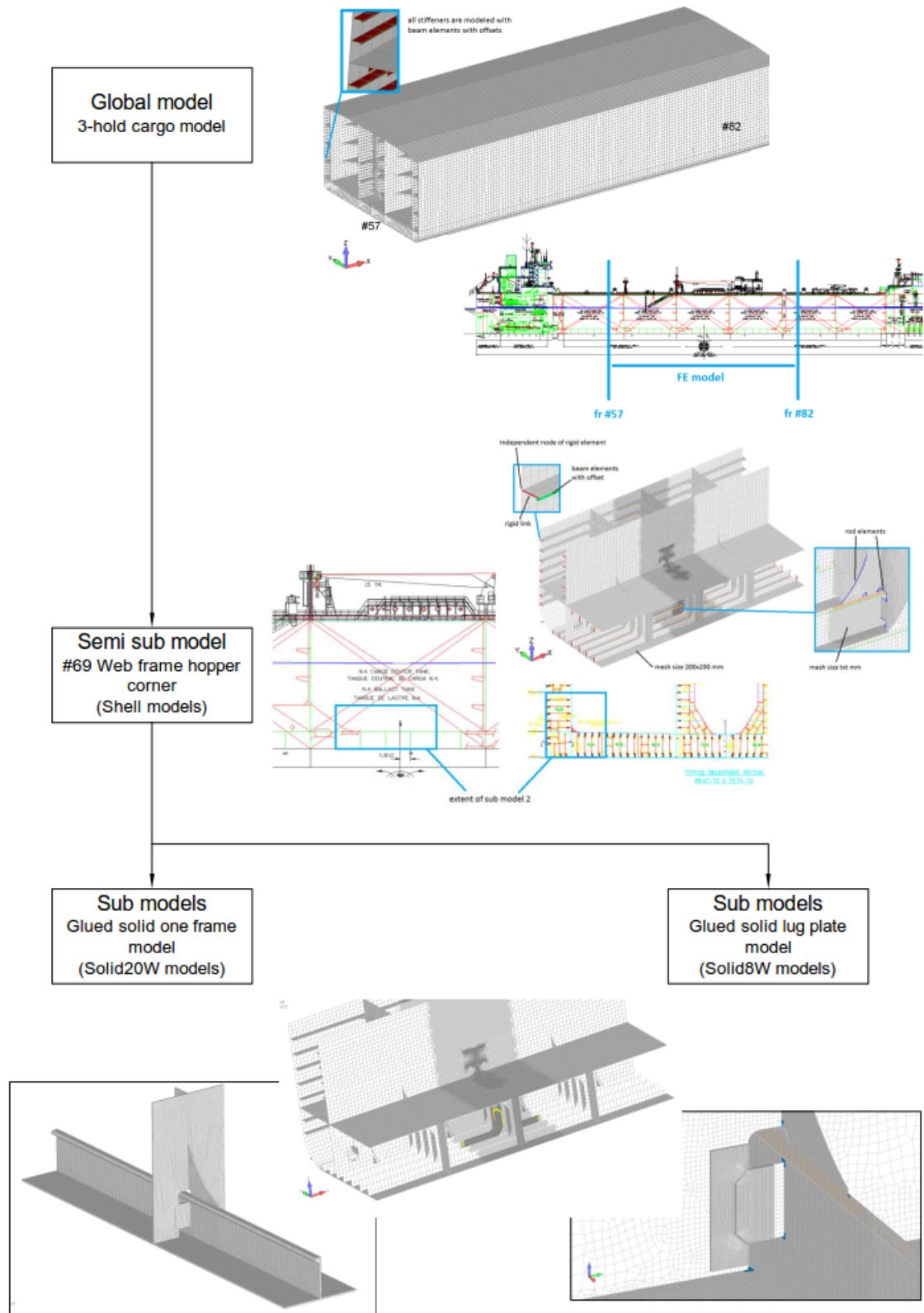


Figure 13. The modeling hierarchy from global models to sub models.

4.2.3 Shell models

The semi sub-models are modeled with the shell elements, which are industry standard in ship design and recommended by classification societies. Therefore, shell models are chosen for comparison of this study. The shell models are labeled with Q8 after the quadratic 8-node element type. There are two different shell element models: Q8 Shell and Q8 Shell Wleg. Actually, the models are same but the derivation of hot spot stresses differ. In the Q8 Shell model the hot spot stress is derived by classical means of hot spot stress extrapolation and in the Q8 Shell Wleg model the weld leg shift is applied as instructed by ABS. This means that extrapolations points are shifted with weld leg length in a quadratic fitting curve. In both models the offset element of the lug plate and web frame are modeled with shell element, thickness of which is equal to two times lug plates thickness, as shown in Figure 1. c). The summary of shell models are presented in Table 2 and part of the model is presented in the Figure 14.

Table 2. Shell models used in this study.

	Q8 Shell	Q8 Shell Wleg
Mesh size ($l \times w$)	$t \times t$	$t \times t$
Element type	8-node	8-node
Note	Offset elem. $2t$	ABS weld leg shift

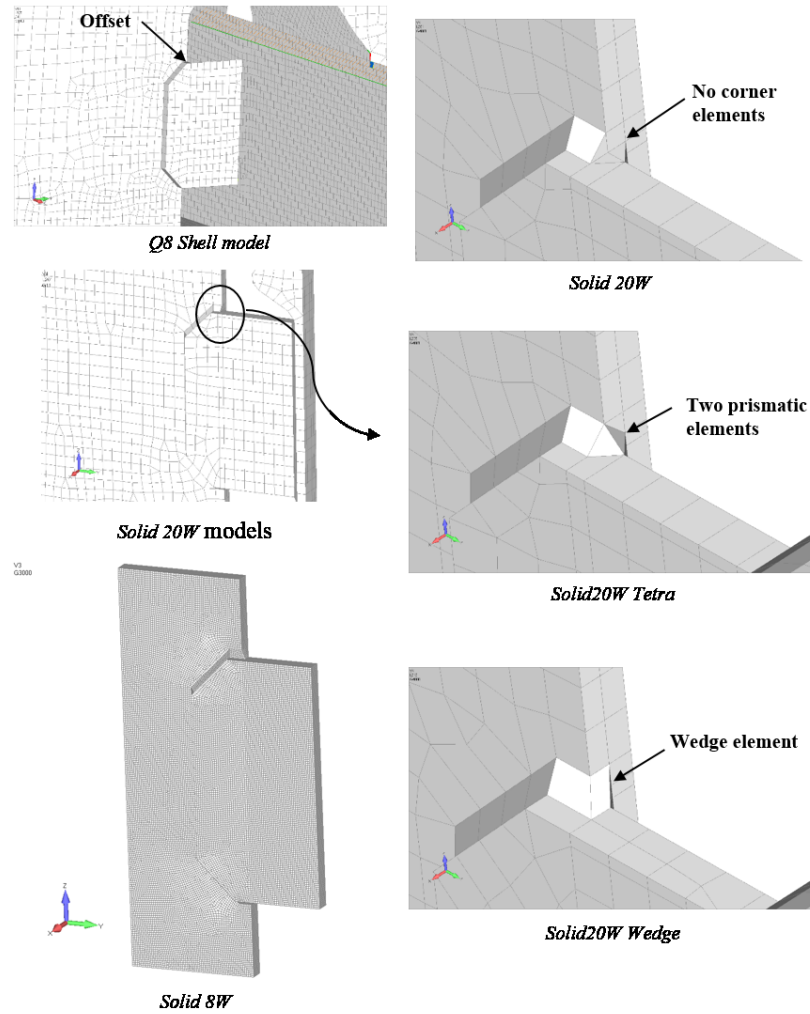


Figure 14. Different shell and solid models.

4.2.4 Solid models

The solid models are not widely used in shipbuilding industry. Solid models represent sub-models in model hierarchy. In this study, solid models are in the main focus to find out if there is any advantage of using solid models in terms of accuracy of results and modeling effort.

The solid models are divided into two main categories according to element type. The solid 20 models are modeled with 20-node parabolic hex elements and solid 8 models are modeled with 8-node linear hex elements. The summary of the models is presented in Table 3 and Figure 14.

Table 3. Used solid models in study.

	Solid20W	Solid20W Tetra	Solid20W Wedge	Solid8W	Solid8W Gap	Solid8W BR
Mesh size (/xwxt)	txtxt/2	txtxt/2	txtxt/2	t/8	t/8	t/8
Elem. type	20-node	20-node	20-node	8-node linear	8-node linear Unconne cted nodes btw. Lug and web	8-node linear
Note	No weld corner	Tetra weld corner	Wedge weld corner	Referenc e model		Reduced bending stress

The solid 20 models were chosen to this study according to Lotsberg's (2006) recommendations. There are 4 different solid 20 models to compare different effects from weld modeling. All the models are constructed from 20-node parabolic hex elements. Solid20W, Solid20W Tetra and Solid20W Wedge represent different approaches of weld modeling. In the Solid20W model the weld corner at hot spot location is not modeled. This reduces the modeling time because there is not that much preparation effort involved to divide the model to parts which suits for hex meshing. This model's weakness is the fact that weld is not realistically modeled. The Solid20W Tetra model has two tetra elements on lug plate weld corners. The tetra element can easily be added to the model and the procedure does not increase the modeling time notably. The disadvantage lies in the fact that tetra element is not good in bending problems. In Solid20W wedge model the weld corner is represented with wedge element. This modeling approach is the most time consuming because the geometry of the model needs to be sliced to smaller parts in order to mesh it with hex elements. The advantage of this model is that there is consistency with elements.

The Solid8W models are the most accurate models used in this study. These models are used as references and base of benchmarking. Also with these models the bending and membrane stress can more easily be extracted. All Solid8W models have linear 8 node hex elements and weld corners are modeled with wedge elements. The Solid8W Gap model has unconnected nodes between lug plate and web frame, see Figure 15. This represents the situation where loads are carried only through the weld. Solid8W BR (bending reduced) differs from other Solid8W models because in the post processing the bending stress is reduced by 40 %.

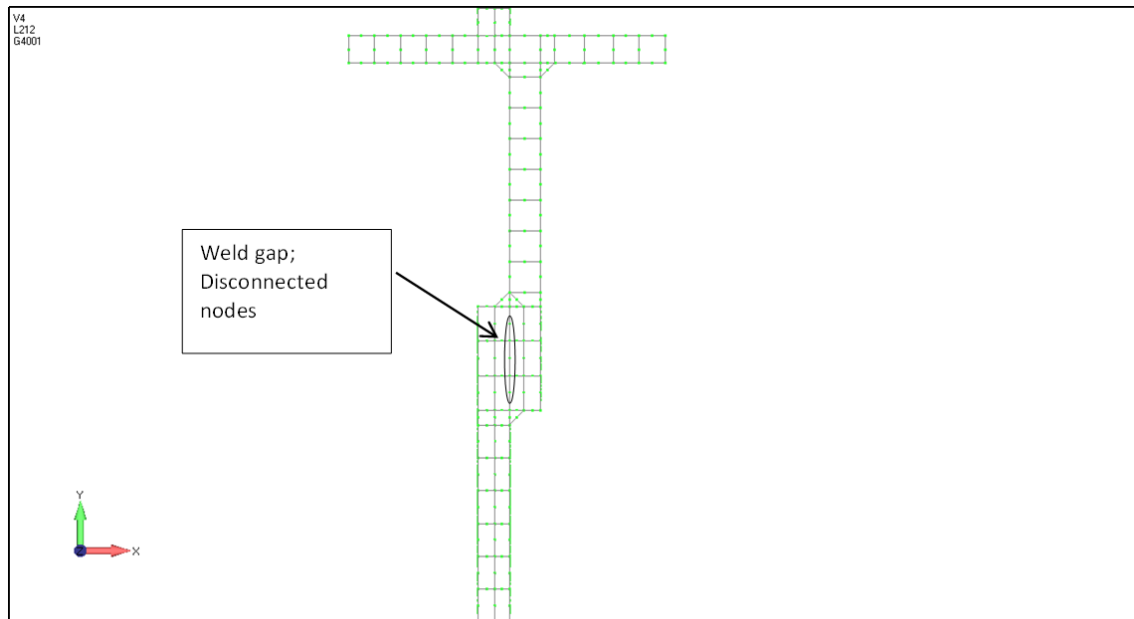


Figure 15. The gap between the lug plate and the webframe is modeled with disconnected nodes.

4.2.5 Loads and boundary conditions

In the stress response calculations all the models have unit loads. Applied unit loads are presented in Table 4. Each unit load represents one component load in the finite element model. For the global model all the unit loads are applied in addition to global loads. For the sub models only the local pressure loads and tank inertia pressure are applied.

The global model has pinned boundary conditions on both ends. In addition, aft end boundary is free to move in longitudinal direction and forward end is restricted in rotation over the longitudinal axis. Global loads are applied on spider node, which is rigidly connected to all longitudinal members. The definition of rigidity is linked to all displacements on every direction of the Cartesian coordinate system but rotations to all directions are left free. This follows procedure given in Lloyd's Register's direct strength analysis document (Lloyd's Register 2012).

Local wave pressure loads cause additional global bending and shear forces. The local and global load responses are solved separately and thus in total response the local load effect must be eliminated in order to achieve realistic stress response. The FEA solver balances element level nodal forces. Based on these balanced forces the additional global forces can be eliminated by means of superposition principle resulting in zero global bending moment, axial and shear force at the calculated cross section in case of local loads.

Table 4. Unit loads used in FEA models.

ID	Load component	Unit load		
1	Vertical bending moment	1 kNm	Global loads	
2	Vertical shear force	1 kN		
3	Lateral bending moment	1 kNm		
4	Lateral shear force	1 kN		
5	EWP FL1	1 kPa	Local wave pressure strip loads	
6	EWP FL2	1 kPa		
7	EWP FL3	1 kPa		
8	EWP FL4	1 kPa		
9	EWP FL5	1 kPa		
10	EWP FL6	1 kPa		
11	EWP FL7	1 kPa		
12	EWP FL8	1 kPa		
13	EWP FL9	1 kPa		
14	EWP FL10	1 kPa		
15	EWP FL11	1 kPa		
16	EWP FL12	1 kPa		
17	EWP FL13	1 kPa		
18	EWP FL14	1 kPa		
19	EWP FL15	1 kPa		
20	EWP FL16	1 kPa		
21	EWP FL17	1 kPa		
22	EWP FL18	1 kPa		
23	EWP FL19	1 kPa		
30	ITP COT acc. in x-direction	1 m/s ²	Tank loads	
31	ITP COT acc. in y-direction	1 m/s ²		
32	ITP COT acc. in z-direction	1 m/s ²		

Local loads caused by external wave pressure (EWP) are divided to smaller strips in order to capture the pressure distribution caused by hydrodynamic pressure (Det Norske Veritas 2010). The pressure in each pressure strip is constant on the longitudinal direction. The wetted surface effect near the waterline level is taken into account according to ABS guidance (American Bureau of Shipping 2014). The pressure strips on port side of the ship are shown in Figure 16. Pressure strips are sized to match RAO data from the seakeeping analysis.

Inertia loads acting in cargo and ballast water tanks are modeled using three separate pressure load cases corresponding to unit surge, sway and heave accelerations at each tank's center of gravity point (American Bureau of Shipping 2014). The pressure is a multiple of a cargo or ballast water density, an acceleration and distance between free surface and calculation point.

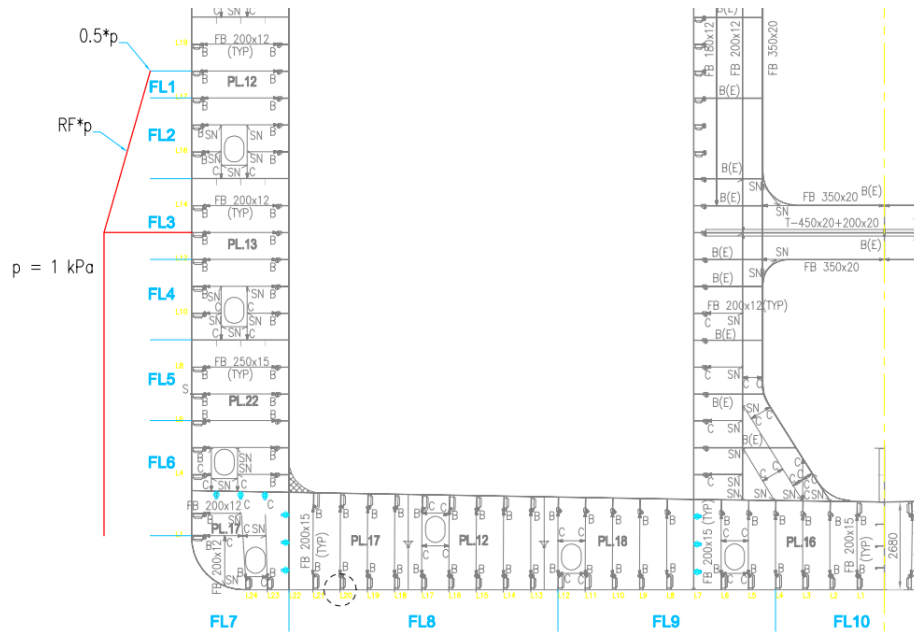


Figure 16. Division of local wave pressure loads. Portside is shown. Starboard side is divided the same way. Water pressure (p) magnitude is 1 kPa. The wetted surface reduction factor (RF) depends on the distance from the water line.

For fatigue assessment the environmental data is needed to calculate actual loads acting on the vessel. The wave scatter information used in this study is presented in Appendix 1. The wave scatter is based on real measured data from the field where FPSO (before conversion) have sailed. In fatigue assessment, the ship's full loading condition is applied.

4.3 Hot spot locations

The hot spot locations of the lug plate connection are presented in Figure 17. The hot spot locations HS3 and HS4 are used in this study. The special interest behind these two locations lies in the fact that both hot spots have offset which has to be modeled with different techniques as presented Figure 1. In addition, the hot spot 4 has been found to show very high fatigue damage.

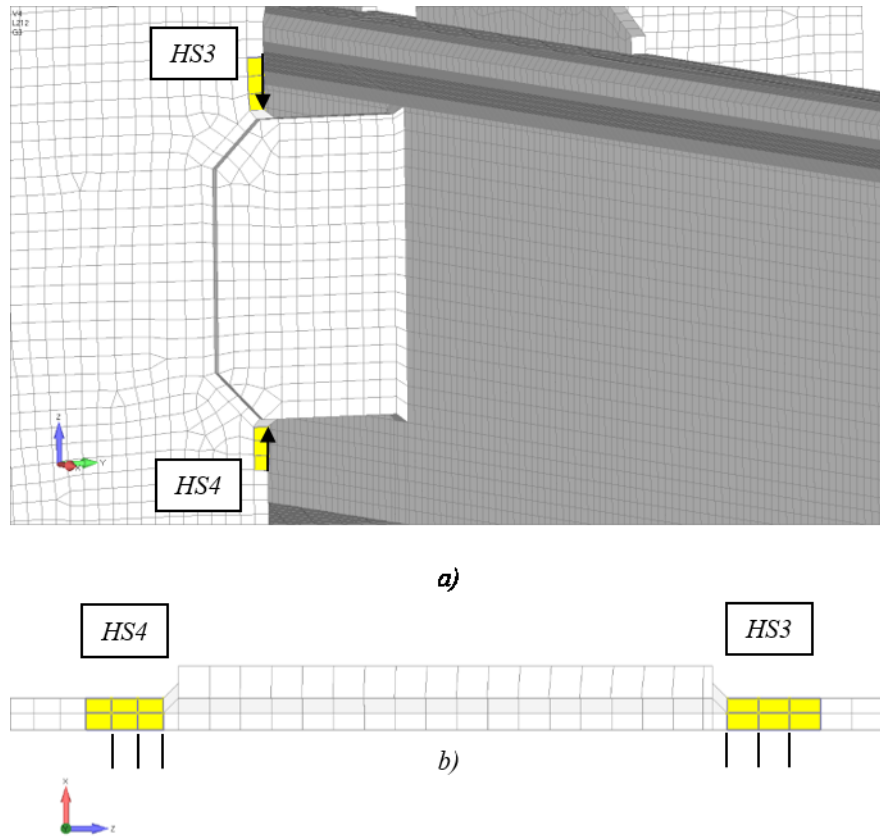


Figure 17 Hot spot locations HS3 and HS4 in Solid20W model are presented with yellow color and extrapolation paths with arrows (a). Through thickness linearization locations are indicated with black lines. Global co-ordinate axes are shown at bottom left corner in both figures.

5 Results

5.1 Fatigue damage

The fatigue damage is calculated with Q8 Shell, Solid20W Tetra, Wedge, Solid8W and Solid8W bending reduction models for hot spot locations 3 and 4. The used stress response factors (SRF) are hot spot stresses calculated with $0.5/1.5t$ extrapolation method. A component stochastic method is used in fatigue calculation and procedure is explained in the chapter 3.4. The loads used in FE models are presented in Table 4. Jonswap wave spectrum is used. The scatter data is presented in Appendix 1. Damages are calculated with design life of 3.105 years, which is the time ship has been in full loading condition

The fatigue damage of Q8 Shell model induced by global loads, tank pressure components and external pressure components are presented in Figure 18. The external pressures are the most significant in the total damage of the lug plate. The next significant is tank pressures. Global loads do not affect so much to the total damage. The same distribution of different load components can be seen also in other models. Thus, those are not shown here.

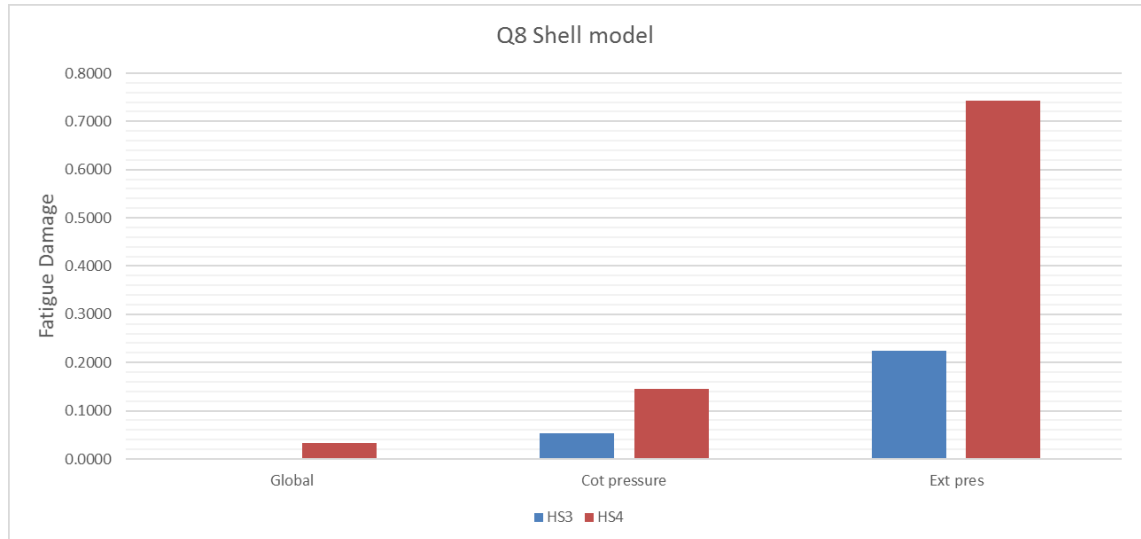


Figure 18. Fatigue damages of different combined component loads at HS3 and HS4.

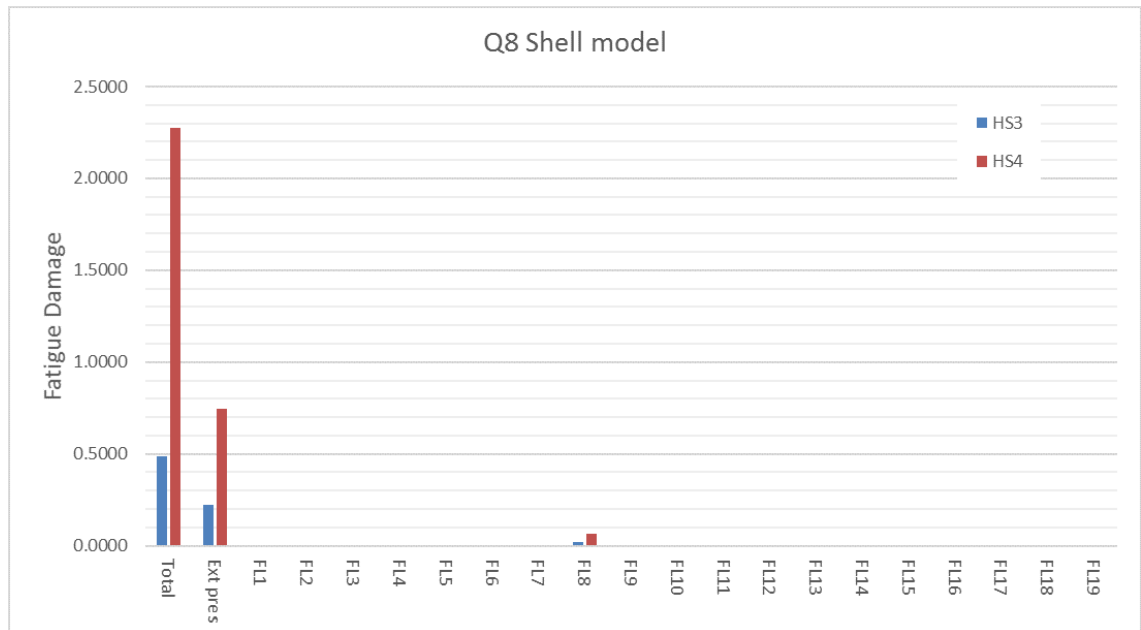


Figure 19. Total fatigue damage, damage induced by all external pressure strips and damage by different external water pressure strips at HS3 and HS4.

The fatigue damage caused by different external water pressure components, total damage and damage from all external pressure strips are shown in Figure 19. The most significant external water pressure strip is FL8, which is on the bottom shell below the lug plate. Thus FL8 was used as load component in structural hot spot stress analysis. Other water pressure strips do not have significant effect on fatigue damage. However, the total damage is also affected by other component loads and is very sensitive to all load components. Therefore, fatigue life of the lug plate cannot be assessed based on only one load component.

The total fatigue damage of different models on HS3 and HS4 is shown in Figure 20. On hot spots 3 and 4 the damage differences are in line with stress concentration factors calculated by extrapolation technique. At hot spot 3, the Solid8W models have the lowest damage and the Q8 Shell model has the highest damage. The Solid20W Tetra has lower damage than Solid20W Wedge model. At hot spot 4, the Solid20W Tetra model has the highest damage. The second highest damage is in the Q8 Shell model and the third highest damage is in Solid20W Wedge model. The Solid8W models have the lowest damage and they are only models, which have total damage level below 1. Difference to others is significant. Damage level below 1 means that Solid8W models are only ones to withstand loading numerically.

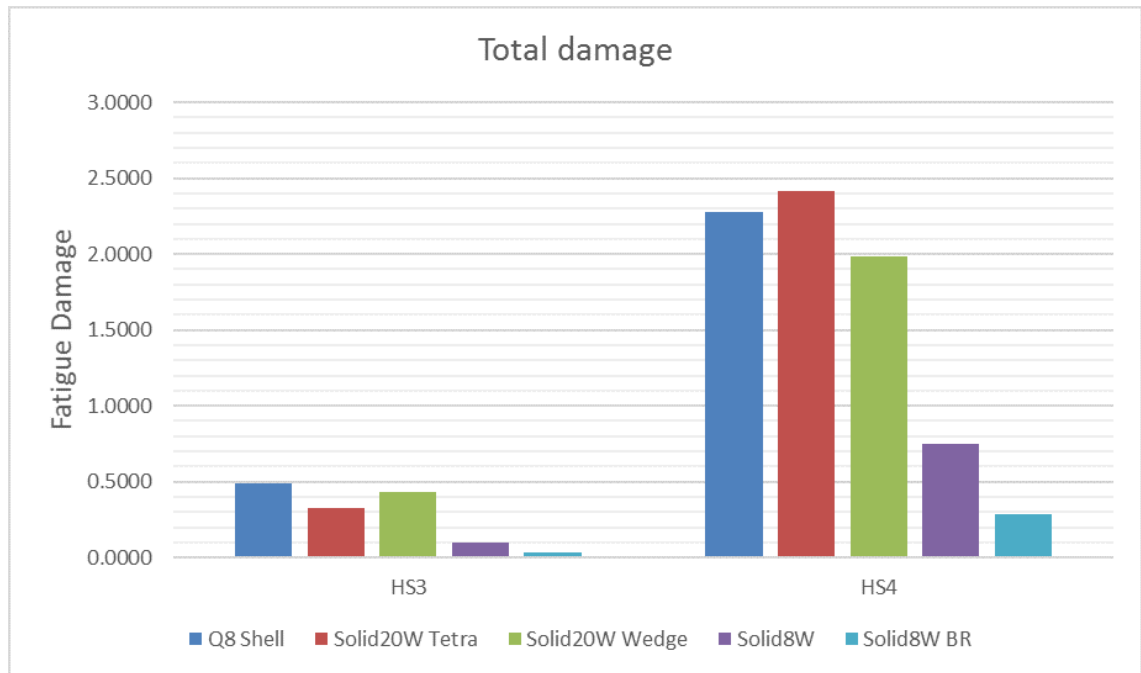


Figure 20. Total fatigue damage of different models at HS3 and HS4.

The total damages can also be expressed by fatigue life. The maximum fatigue life can be transformed from total damage by dividing the used design life (3.105) with the damage. The maximum design lives at HS3 and HS4 are shown in Figure 21 and Figure 22 respectively.

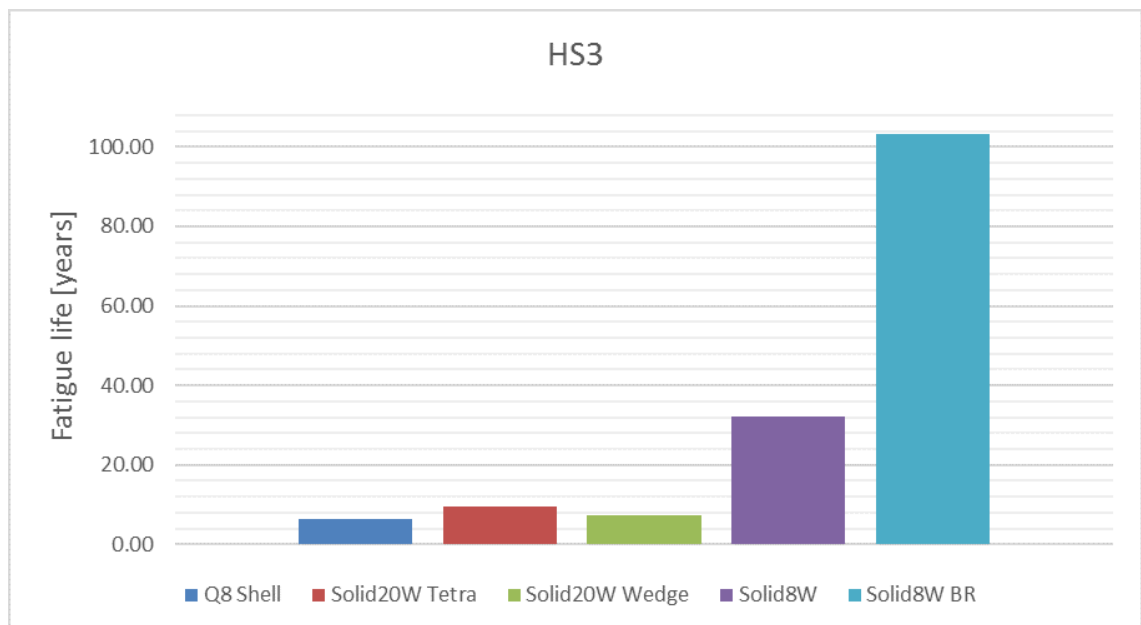


Figure 21. The maximum fatigue life of different models at HS3.

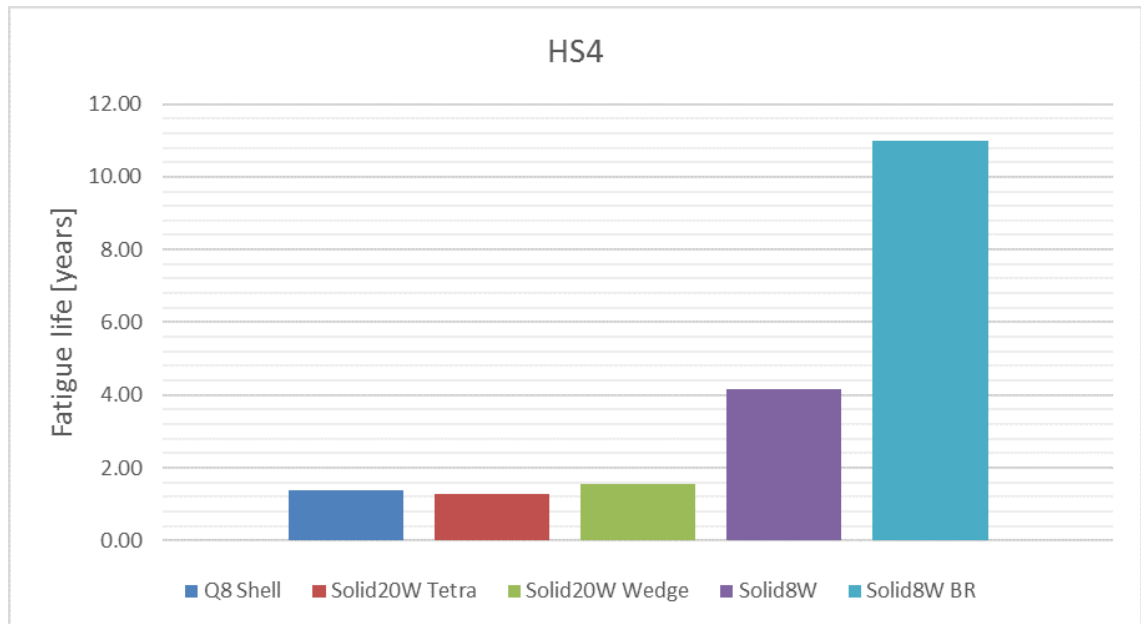


Figure 22. The maximum fatigue life of different models at HS4.

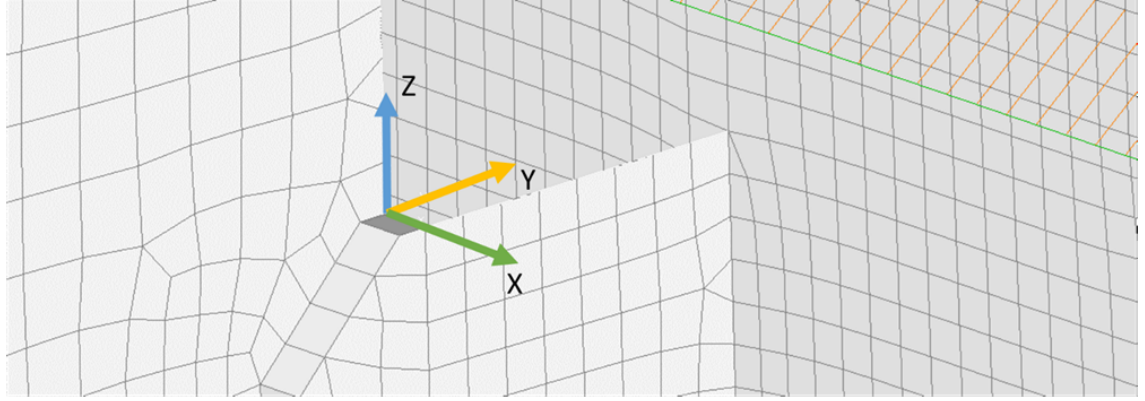
The fatigue life calculated with Solid8W model is more than 30 years at HS3. Solid8W BR model have higher fatigue life than 100 years. Shell model and other solid models have fatigue life less than 10 years. At HS4, none of the models have higher fatigue life than 25 years, which is design life for FPSO. Solid8W BR has highest fatigue life with over 10 years. The Solid8W has fatigue life higher than 4 years. The Q8 Shell model and other solid models have lower fatigue life than 2 years.

5.2 Deformation and stress response of the lug plate connection

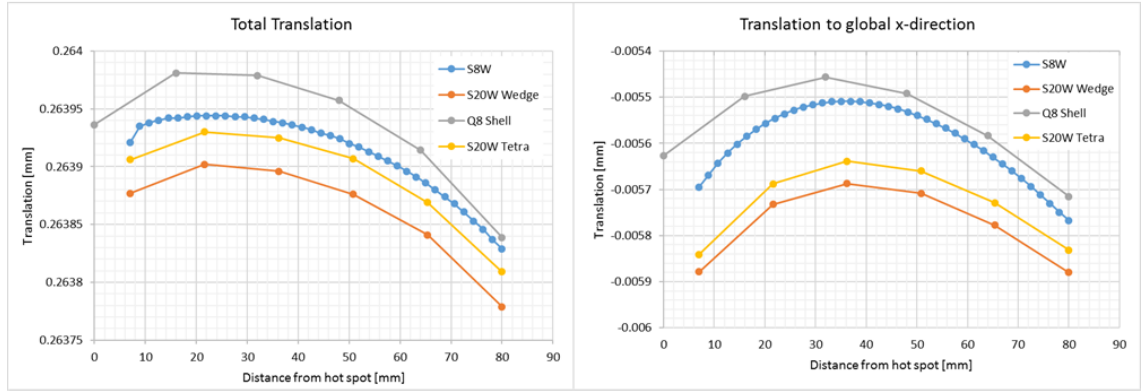
The deformation is studied on the top surface of the lug plate connection towards HS3, see Figure 23. The used load is pressure strip EWP FL8 below the lug plate on the bottom surface of the shell plating. Magnitude of pressure is 1 kPa .

In Figure 23, the translations of nodes by global co-ordinates towards HS3 on top surface at free edge are shown. Because the translations are checked on top surface of the solid elements and the shell model gives translations on mid-plane, translations of the shell model are to be corrected to the top surface. This can be done using trigonometric functions and taking into account the rotations on nodes and half-thickness of element. The total translation is achieved with basic vector calculus. This is justified because the solution of FEA is based on linear theory and hence on small displacements.

The deformation shapes of all models are almost equal. In Solid8W model translations to global X -direction and global Z -direction are stronger compared to other models at the weld toe. This highlights the phenomenon of local stiffness increase of the weld. From translation figures the stiffness of different models can be seen. The two element layer element presentation of Solid20W models is stiffer compared to shell element model and Solid8W model, which has 8 element layers. Especially, the stiffness of Solid20W model to global X -direction is higher. This means that Solid20W models do not take into account the bending of the plate as accurately as shell and Solid8W model do. In global Y -direction all the models have almost the same displacement due to the fact that there is no load in Y -direction. Interesting is the difference of displacements between Solid20W Wedge and Solid20W Tetra models. Only one element difference on weld corner affects the overall stiffness clearly. The Solid20W Tetra model is closer to the Solid8W model stiffness. The same behavior of different models can be seen, when the deformations are checked at mid-planes.

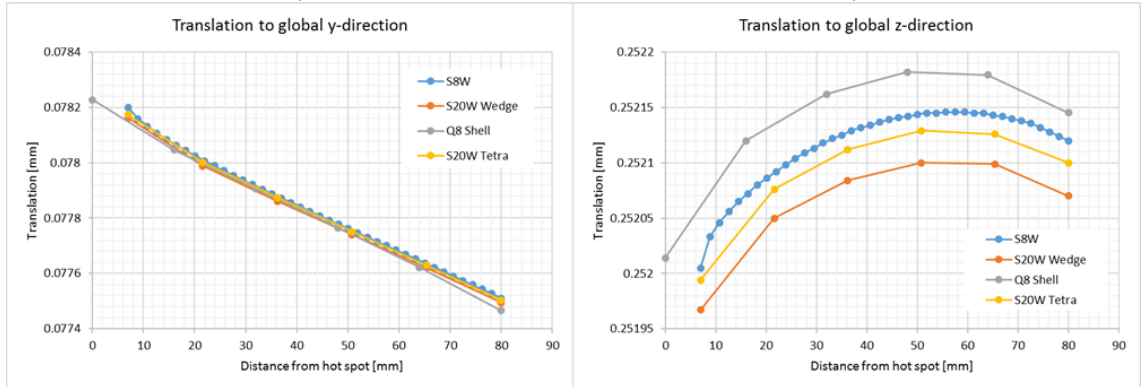


a)



b)

c)



d)

e)

Figure 23. Comparison of translation components of different models on upper edge of HS3 and co-ordinate directions (a). b) total translation c) translation to global X-direction d) translation to global y-direction e) translation to global z-direction.

Deformations of lug plate models Q8 Shell, Solid20W Wedge, Solid8W models are presented in Figure 24, Figure 25 and Figure 26, respectively. More figures are presented in Appendix 2 to clarify the deformation shapes. It can be seen that lug plate rotates around global Y- and Z-axes. Thus it can be concluded that the lug plate is bending at HS3

and HS4 locations. Also shear deformation can be seen and how the longitudinal stiffener and bracket on top of it prevents the deformation in global Z-direction.

The contour plot in Figure 24, Figure 25 and Figure 26 is maximal principal stress. It can be seen that the stress concentrations of all models are more or less at the same locations. The maximum principal stresses on model Q8 Shell and Solid20W Wedge are 2.561 MPa and 2.753 MPa respectively. These are almost on the same level. In Solid8W model, the maximum principal stress is 3.79 MPa . Big difference is due to denser mesh, which increases the stress peak at the hot spot. The peak stress increase is also shown in Figure 33.

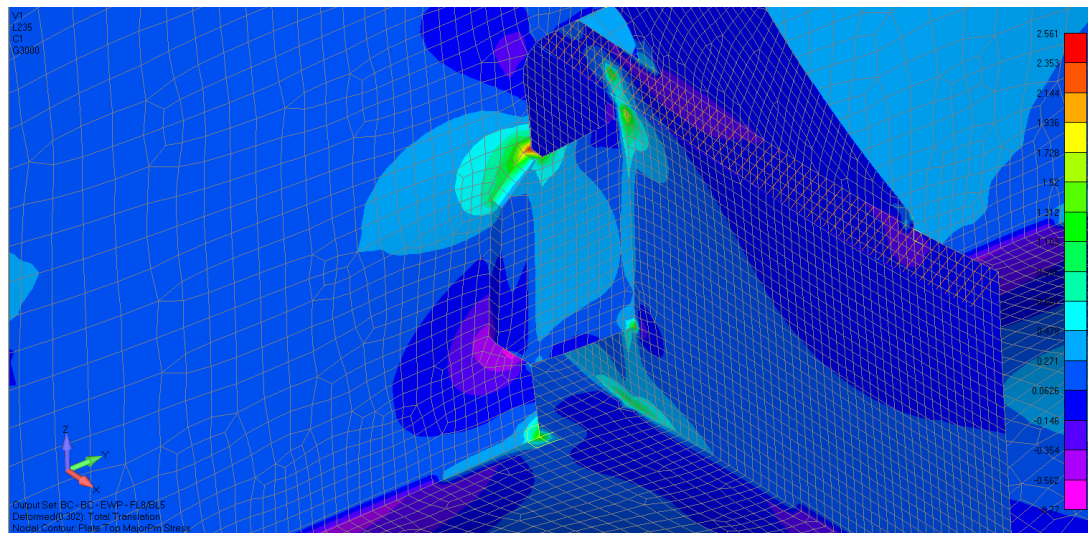


Figure 24. Plot of deformed Q8 Shell model. Deformation is scaled by 5. Contour is based on non-averaged nodal maximum principal stress. Only part of the model is shown.

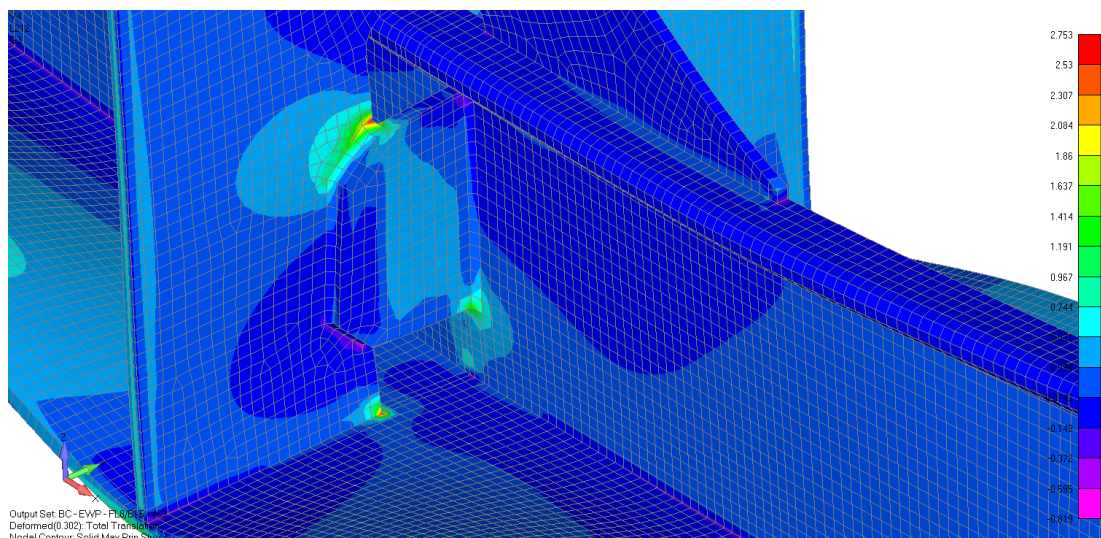


Figure 25. Plot of deformed S20W Wedge model. Deformation is scaled by 5. Contour is based on non-averaged nodal maximum principal stress. Only solid elements are shown.

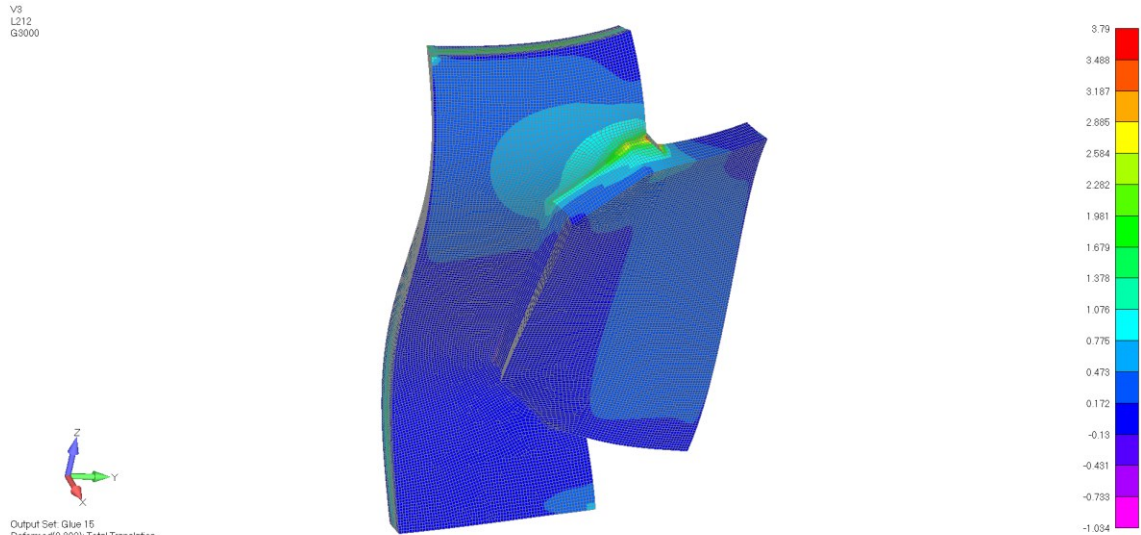


Figure 26. Plot of deformed Solid8W model. Deformation is scaled by 5. Contour is based on non-averaged nodal maximum principal stress. Only solid elements are shown.

The effect of weld modeling on the peak stress location and stress magnitude is shown in figures 28 to 31 at HS3 location. When the weld corner element is not modeled the peak stress location is on the top of the lug plate not at the weld toe. This is clearly wrong behavior because the stress peak should be at the weld toe, where the crack usually initiates. Therefore, Solid20W model is not suitable to analyze structural hot spot stress at the weld toe. In Solid20W Wedge model the stress peak is more concentrated to weld corner compared to Solid20W Tetra model. The high stresses are more widely spread along the weld and top face of the lug plate in Solid20W Tetra model. The Solid20W Wedge model can separate the lug plate's back face weld stress concentration better than the Solid20W Tetra model. In the Q8 shell model the stress distribution and stress peak concentration location is closer to Solid20W Tetra model than wedge model. The Q8 Shell model cannot separate stress peak from lug plate's back face weld concentration and have only one stress concentration point. For these reasons, the Solid20W Wedge model can determine the peak stress concentrations closer to realistic situation.

Non-averaged nodal maximum principal stresses in Solid20W, Solid20W Tetra and Solid20W Wedge are 2.692 MPa , 2.589 MPa and 2.753 MPa respectively. In Q8 Shell model the maximum principal stress is 2.561 MPa . The wedge corner element model stress results deviates from the tetra model, because stress peak is more concentrated to weld corner.

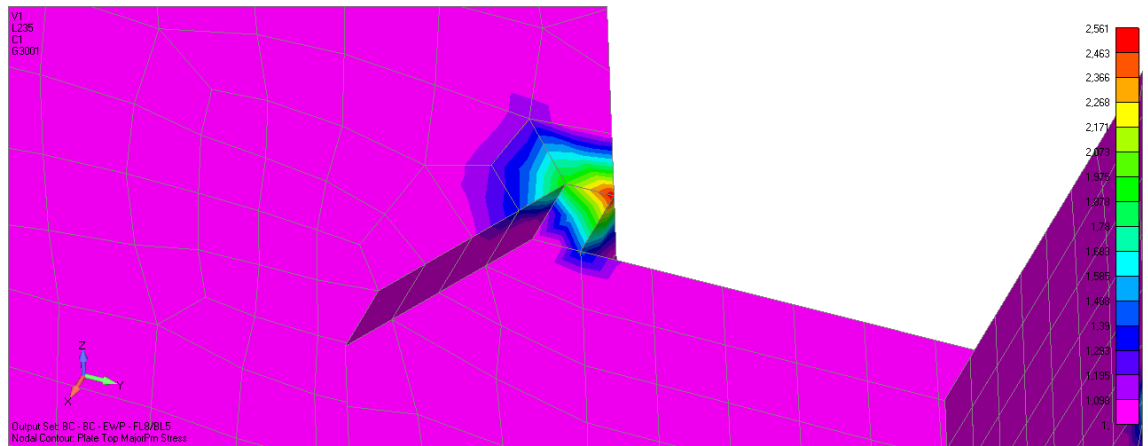


Figure 27. The maximum principal stresses in Q8 Shell model at HS3. Offset is modeled with shell element which has thickness of two times the lug plate thickness.

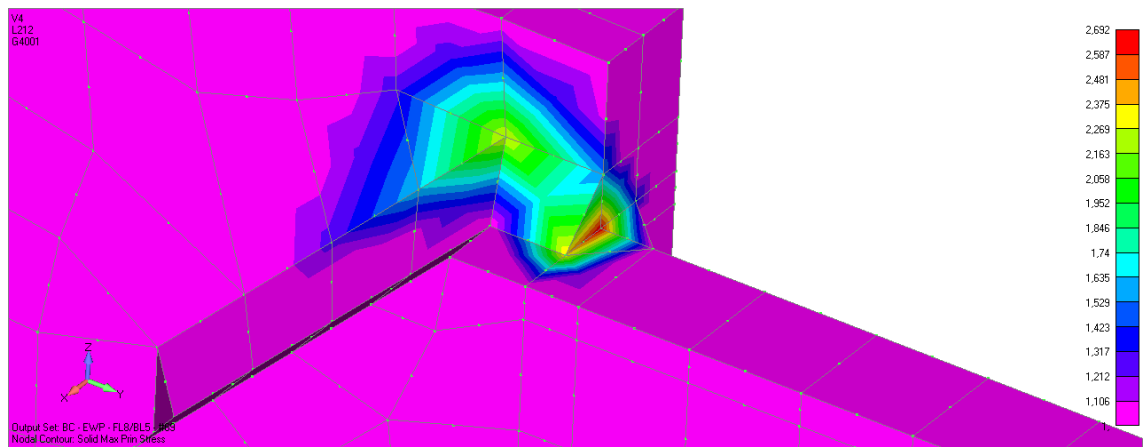


Figure 28. The Solid 20W model without weld corner elements.

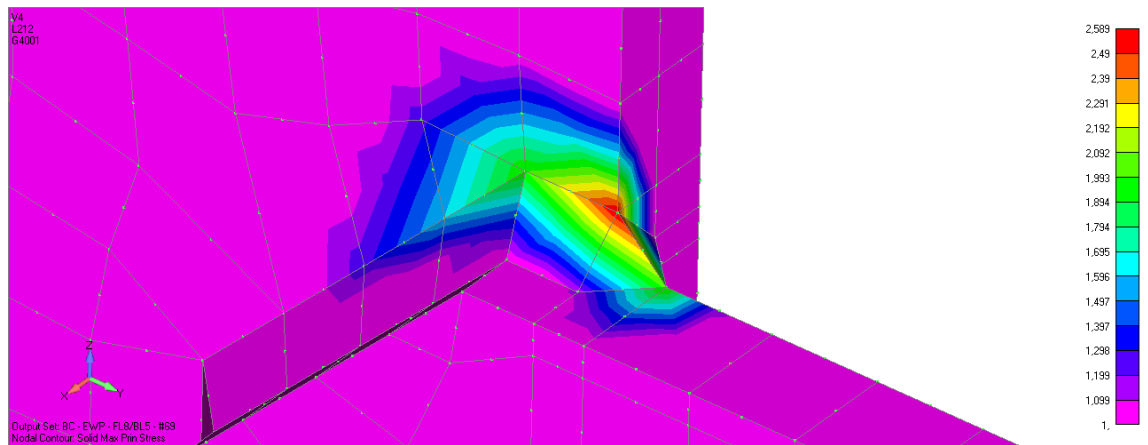


Figure 29. The Solid 20W Tetra model. Weld corner is modeled with two tetra elements.

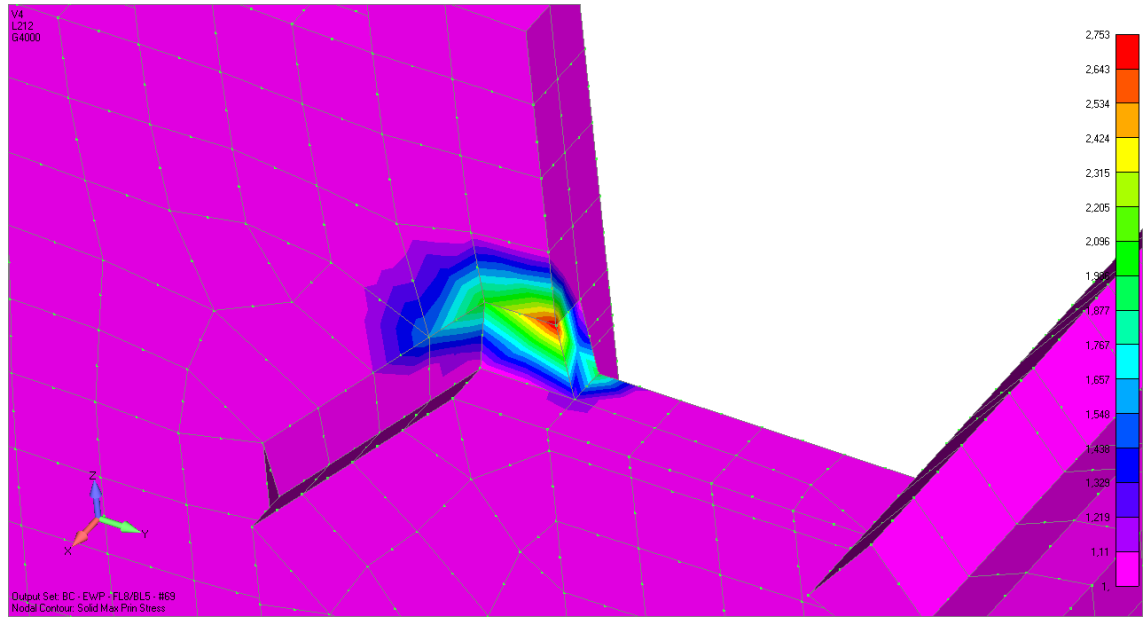


Figure 30. The Solid 20W Wedge model. Weld corner is modeled with wedge element.

5.3 Structural hot spot stresses

In this section the different models are studied on the structural hot spot stress level. The used load is pressure from the strip EWP FL8 below the lug plate on bottom surface of the shell plating. Magnitude of pressure is 1 kPa . The hot spot locations are presented in Figure 17. The extrapolation is done on the free edge of the webframe towards the weld. Extrapolation procedure is introduced in chapter 3.3.1. The derivation procedure of structural hot spot stress by through thickness linearization is presented in chapter 3.3.2.

The extrapolated structural hot spot stresses at hot spot 3 are presented in Figure 31. The Q8 Shell model has the highest hot spot stress. Weld leg correction reduces the stress level below the stress levels achieved from Solid20W models. The Solid20W Wedge model has higher hot spot stress compared to Solid20W Tetra model. The difference is due to higher stress concentration of Solid20W Wedge model at the weld toe. The higher stress concentration affects to quadratic curve fitting increasing the hot spot stress. The hot spot stresses are remarkably lower in Solid8W models compared to other models. The gap between the lug plate and the webframe has only small effect on hot spot stress. This is in line with Wang's (2008) observations. The bending reduction decreases hot spot stress remarkably.

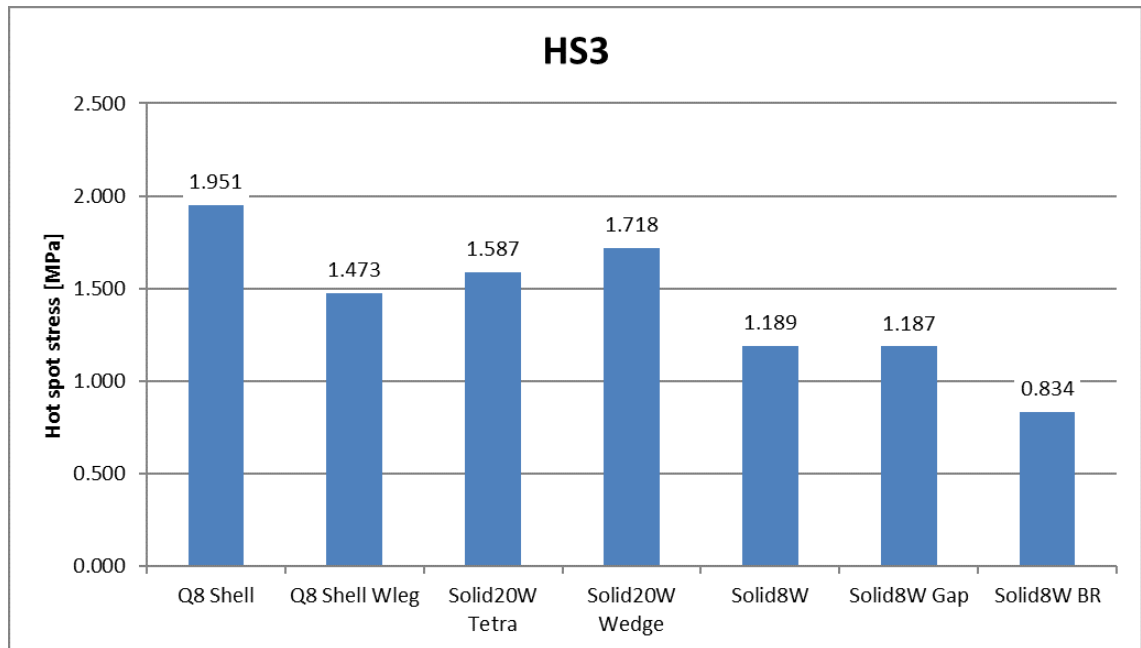


Figure 31. Extrapolated structural hot spot stresses at HS3 on different models. Stresses are presented in global co-ordinate system.

The extrapolated structural hot spot stresses at hot spot 4 are presented in Figure 32. The Solid20W Wedge model has the highest structural hot spot stress. The Q8 Shell model has the second highest hot spot stress and weld leg correction reduces the stress level close to stress level achieved from Solid8W model. The gap model does not affect the hot spot stress as it did not in case of HS3. The bending reduction model gives the lowest hot spot stress level. The interesting result is that Solid20W Wedge model has lower hot spot stress compared to the Solid20W Tetra model. In case of HS3 the results are vice versa. This can partly be explained by the fact that stress ROPs of the Solid20W Wedge model deviates from the Solid20W Tetra model and other models remarkably. The stress ROP's at HS3 and HS4 are presented in Table 5 and Table 6 respectively. Apparently the quadratic curve fitting does not compensate the mesh inconsistency.

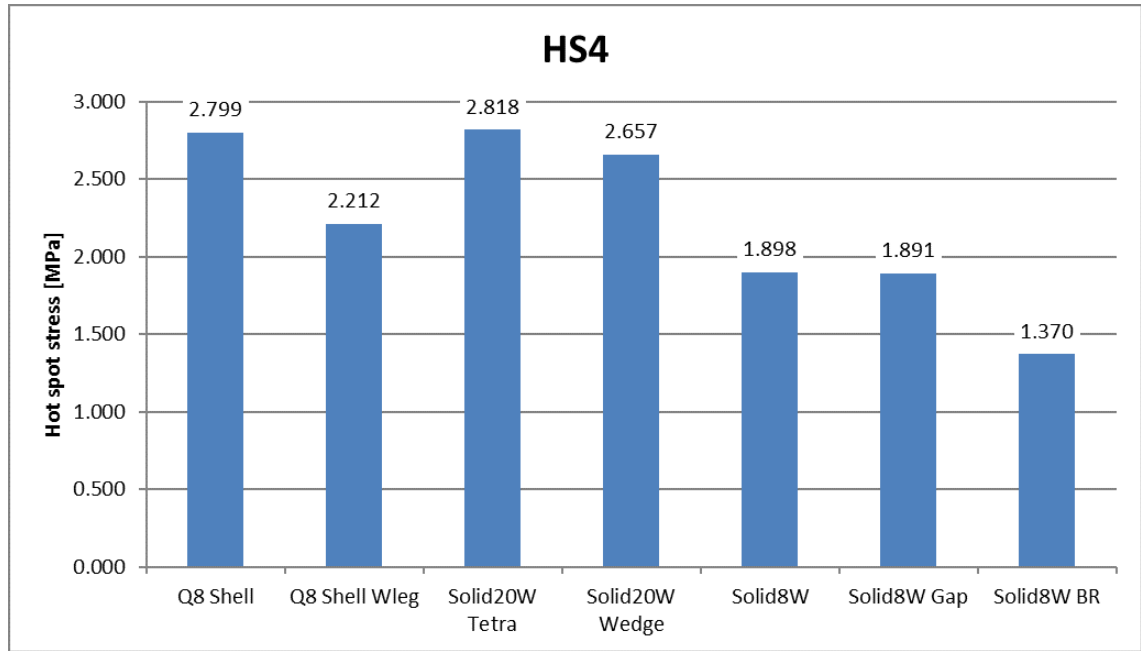


Figure 32. Extrapolated structural hot spot stresses at HS4 on different models.

Table 5. The relative distances of stress ROPs of different models at HS3.

Q8 Shell	Solid20W Tetra	Solid20W Wedge	Solid8W
x/t	x/t	x/t	x/t
0.00	0.00	0.00	-
1.07	0.97	0.97	0.5
2.13	1.95	1.95	1.50

Table 6. The relative distances of stress ROPs of different models at HS4.

Q8 Shell	Solid20W Tetra	Solid20W Wedge	Solid8W
x/t	x/t	x/t	x/t
0.00	0.00	0.00	-
0.95	0.94	0.81	0.5
1.90	1.89	1.62	1.50

The surface stresses normal to weld toe do not deviate a lot between different models further than $1t$ from the weld toe at HS3 and HS4. This can be seen in Figure 33 and Figure 34. The Q8 Shell model has the highest stress at ROPs. The stress peak is the highest in Solid8W model. This is due to denser mesh. The peak stress increases when the mesh density is increased. The peak stresses of Q8 Shell model and Solid20W models are about the same. Solid8W Gap model stress distribution is left out from figures, because it is almost identical with Solid8W model.

The structural stress acquired by through thickness linearization deviate from extrapolated stresses especially in Solid8W model. Difference in Solid20W models is not

that significant. At HS4 same phenomenon can also be seen, but the difference between the Solid20W models increases. The structural hot spot stresses calculated by through thickness linearization are higher on all models. The structural hot spot stress should be same regardless of used hot spot derivation method, see Figure 2. One reason for deviation of structural hot spot stress results might be the hot spot location. The hot spots locate on the free edge of the plate and thus there might be local stress disturbance. Also the extrapolation method could be questioned. It is hard to distinguish is the free edge location closer to extrapolation case a) or b) in Figure 3.

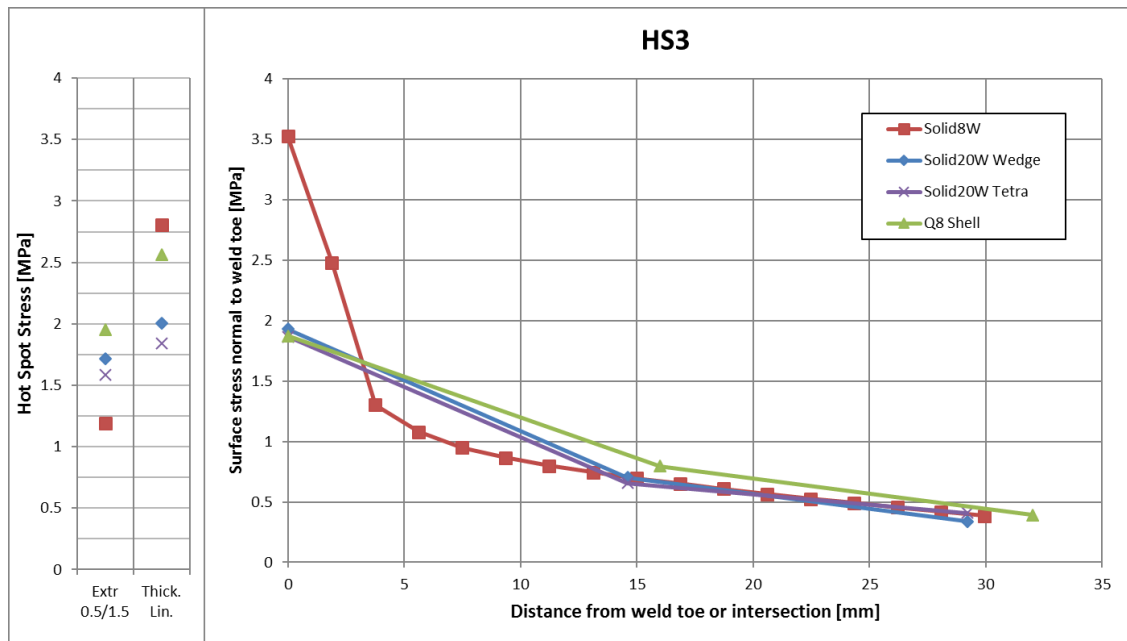


Figure 33. On the left hand side are extrapolated and thickness linearized hot spot stresses at HS3. On the right hand side are surface stresses of different models.

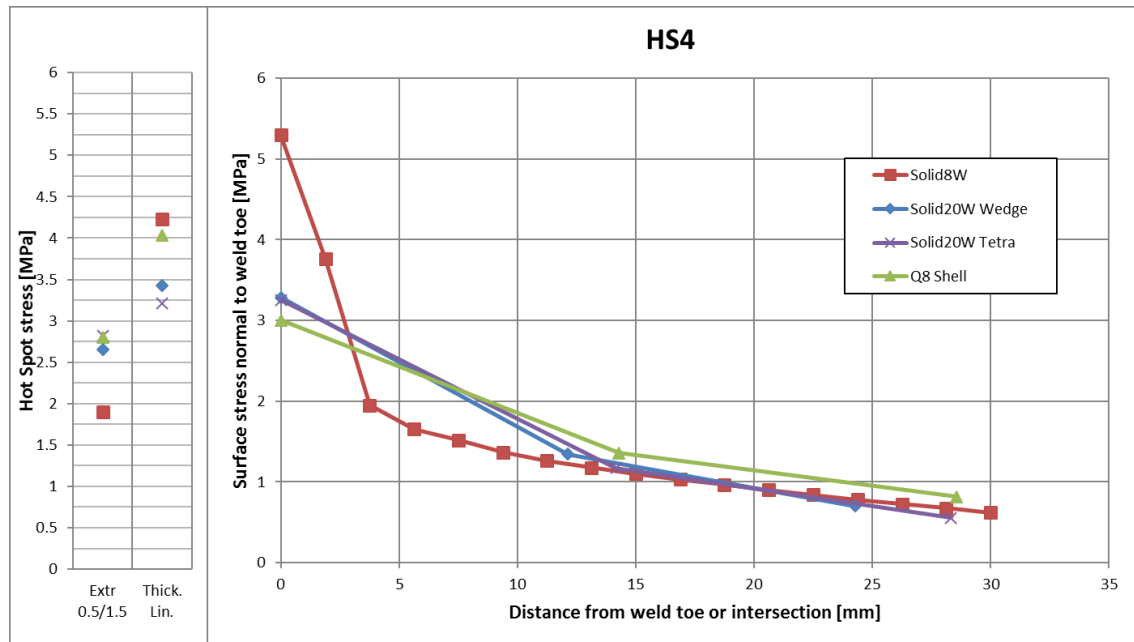


Figure 34. On the left hand side are extrapolated and thickness linearized hot spot stresses at HS4. On the right hand side are surface stresses of different models.

5.4 Through thickness stress distribution

Through thickness stress distributions of Solid8W and Solid20W Wedge models are shown in Figure 35. The used load is pressure strip EWP FL8 below the lug plate on bottom surface of the shell plating. Magnitude of pressure is 1 kPa .

The through thickness stress distribution deviates most at the weld leg location, where the stress peak occurs. Due to stress peak the stress is not linear at the weld toe location. The Solid8W can better capture the stress peak because it has more elements in thickness direction. Non-linear 20-noded solid elements (Solid20W models) should also be able to capture deep stress gradients according to Lotsberg (2006). It can be seen from results that linearized stress in Solid20W deviates from Solid8W model. Therefore, Solid20W model is not able to capture stress gradient as well as Solid8W model.

Beginning from $1t$ distance from weld toe the stress distribution over plate thickness start to be consistent between Solid20W Wedge model and Solid8W model. Also the magnitudes of stresses are quite the same level in both models.

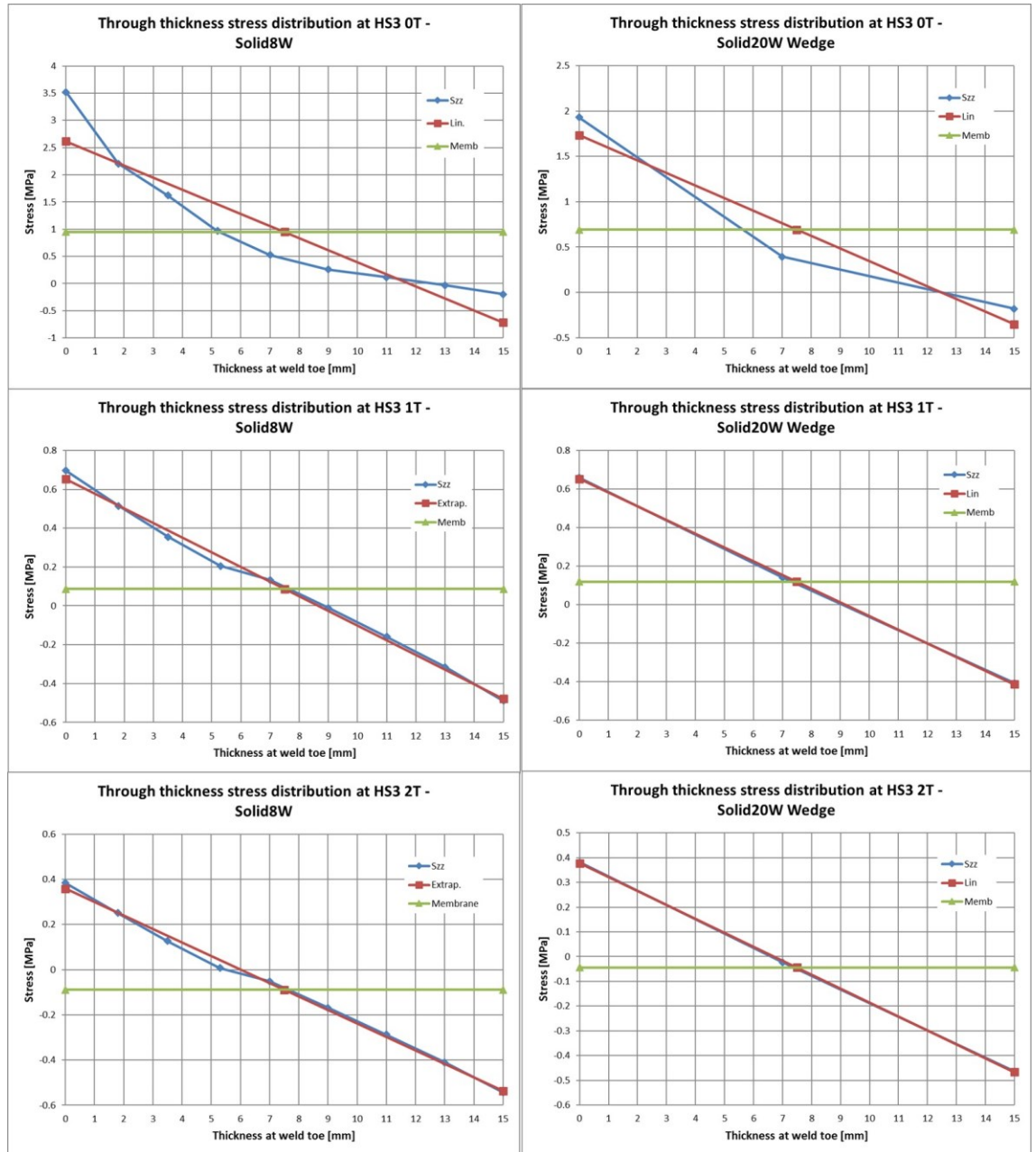


Figure 35. Through thickness stress distributions of Solid8W model and Solid20W Wedge model. Red line represents linear stress distribution, Stress component normal to weld (S_{zz}) is represented by blue line and membrane stress by green line.

In order to take closer look at when the stress gradient changes to linear at HS3, the stress gradients from Solid8W model are shown at distances $0.5t$ and $1.5t$ from the weld toe. Also the stress field at the extrapolation points can be seen. Stress field is shown in Figure 36. The stress field is almost linear already at $0.5t$ distance from the weld toe and the non-linear stress peak is vanished. The stress field remains linear farther from the weld toe. Stress field is also very bending dominant.

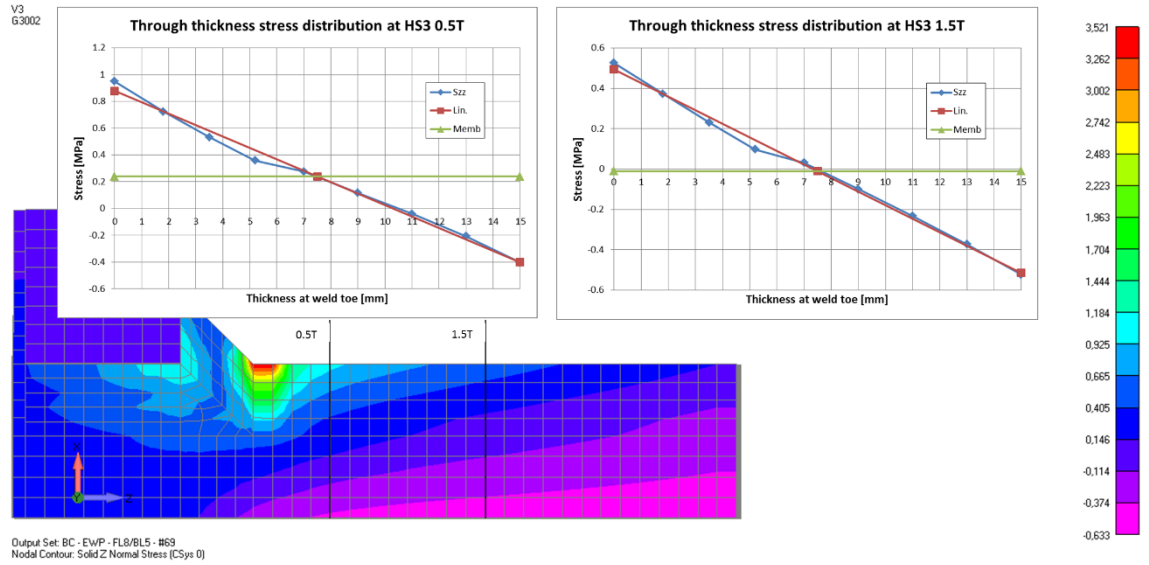


Figure 36. Linearized stresses of Solid8W model at HS3. The stress component (S_{zz}) normal to weld is shown on lug plate connection.

5.5 Membrane and bending stress

Membrane and bending stresses at different locations from HS3 are studied in this section. Membrane and bending stresses are calculated from stress component normal to the weld toe. It is not meaningful to study HS4, because mesh size deviates too much between different models. The used load is restricted to pressure strip EWP FL8 below the lug plate on bottom surface of the shell plating. The membrane and bending stresses of models at different locations from the weld toe are presented in Table 7. Bending to membrane ratio is presented in Table 8.

Table 7. Membrane (σ_{mem}) and bending (σ_{ben}) stresses of different models at different locations from HS3.

x/t	Q8 Shell		Solid20W Tetra		Solid20W Wedge		Solid8W	
	σ_{mem} [MPa]	σ_{ben} [MPa]	σ_{mem} [MPa]	σ_{ben} [MPa]	σ_{mem} [MPa]	σ_{ben} [MPa]	σ_{mem} [MPa]	σ_{ben} [MPa]
0	1.11	0.76	0.63	1.02	0.69	1.04	0.95	1.67
0.5							0.24	0.64
1	0.16	0.63	0.07	0.54	0.12	0.53	0.09	0.57
1.5							-0.01	0.50
2	-0.06	0.46	-0.03	0.49	-0.04	0.42	-0.09	0.45

Table 8. Bending (σ_{ben}) to membrane (σ_{mem}) stress ratio at different locations from HS3.

	Q8 Shell	Solid20W Tetra	Solid20W Wedge	Solid8W
x/t	$\sigma_{ben}/\sigma_{mem}$	$\sigma_{ben}/\sigma_{mem}$	$\sigma_{ben}/\sigma_{mem}$	$\sigma_{ben}/\sigma_{mem}$
0	0.69	1.61	1.51	1.75
0.5				2.68
1	3.93	7.63	4.47	6.47
1.5				-47.86
2	-7.08	-19.21	-9.53	-5.01

The Q8 Shell model behavior deviates from solid models at the weld toe location. In solid models the bending stress is dominant and in Q8 Shell model the membrane stress is dominant. In Q8 Shell model the weld representation with offset element apparently changes the element behavior and therefore membrane stress is dominant. Solid8W model has higher bending and membrane stress at the weld toe compared to Solid20W models. It can be concluded that two elements in thickness direction is not enough to study bending and membrane stress magnitudes at the weld toe. Also one may doubt if the 8 elements in thickness direction is enough, but Goyal (2015) claims that 4 linear elements is enough. To have absolute certainty, denser meshes should be studied.

Farther from the weld toe, more consistency between the different models is reached. The bending to membrane stress ratios increase until $1t$ distance is reached. The membrane stress is changed to negative at about $1.5t$ location and it is increasing farther from the weld toe. It can be concluded that at the weld toe location high local bending is present. The deviation of membrane and bending stress ratio of Solid20W Tetra model at $2t$ distance is due to small membrane stress level.

It can clearly be concluded that the lug plate has high local bending at the hot spot location. For this reason, it is meaningful to compare hot spot stresses with bending stress reduction. The bending stress reduced hot spot stresses along the extrapolated and thickness linearized hot spot stresses at HS3 are presented in Figure 37.

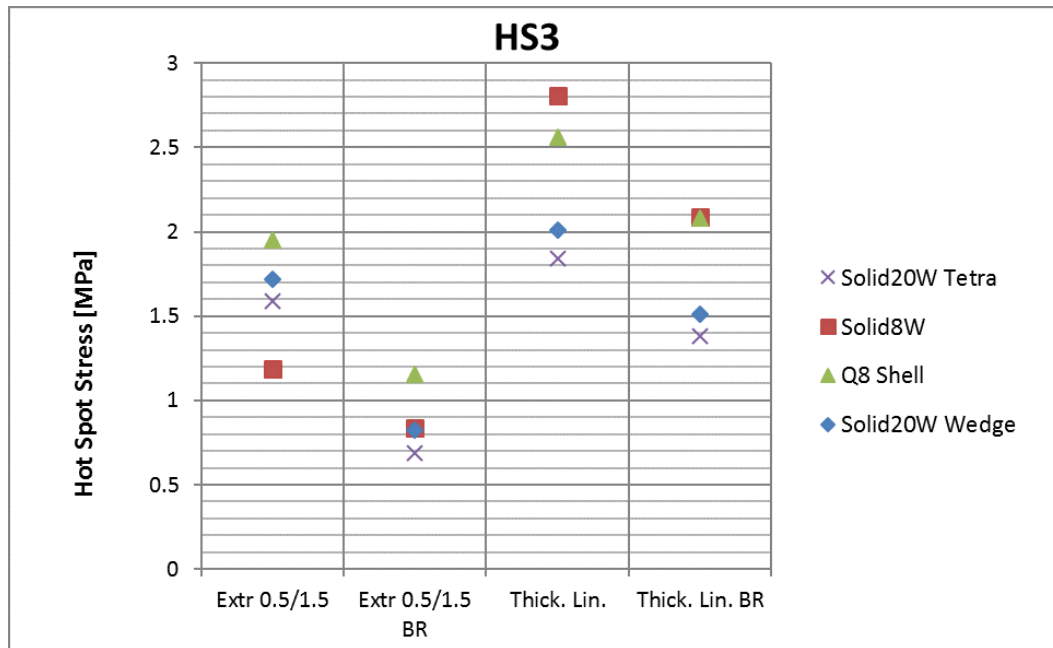


Figure 37. All hot spot stresses of different models at HS3. Different methods from left to right are extrapolation method, bending reduced extrapolation method, thickness linearization method and bending reduced linearization method. BR refers to bending reduction.

The deviation between bending reduced extrapolated hot spot stresses of solid models is much smaller compared to normally extrapolated hot spot stresses. The Q8 Shell model stress deviates due to lower bending stress at the weld toe. The consistency between hot spot stress results of solid models is partly affected by the fact that extrapolated stresses are derived from through thickness linearized surface stresses. The hot spot stress level of all bending reduced models is lower compared to all other methods.

The thickness linearized bending reduced hot spot stresses have wider scatter compared to bending reduced extrapolation hot spot method. Hot spot stress of Solid8W model and Q8 Shell model are almost the same. The hot spot stresses of Solid20W models are lower compared to normally extrapolated method.

6 Discussion

The lug plate has local bending and shear deformation when it is loaded by unit pressure from bottom of the ship. This behavior can be seen from all FE-models used in this thesis. All models have the same deflection shapes, but the stiffness of models is different. The stiffest model is Solid20W Wedge and the most flexible model is Q8 Shell. Stiffness of Solid20W models is due to two elements in thickness direction. The tetra weld corner representation reduces overall stiffness of lug plate connection. None of the models have same stiffness as Solid8W model, except in Global Y-direction, where all models show consistent stiffness. The Q8 Shell model is too flexible and Solid20W models are too stiff compared to Solid8W model. Even though all the models have same load, the stiffness is not exactly comparable because the geometry changes a little bit between models due to modeling simplifications. Also in Solid8W model, the model size is so small that the longitudinal stiffener is not modeled with 3D elements but shell elements and beam elements. This may make the Solid8W more flexible compared to Solid20W models at the hot spot location.

The external water pressure is the major load component in total fatigue damage. The FL8 pressure strip among the external water pressure strips is the most significant load component. Thus the structural hot spot stress analysis results are presented based on this load and total damages of different models are in line with the structural hot spot stress results. The total damage results of Q8 Shell, Solid20W Wedge and Tetra models show higher damage than 1 at HS4 and therefore fatigue cracks should occur. The damages were calculated to real case FPSO conversion using the site-specific data with the real history of the ship. In the sailing history the damage calculation concentrated to tanker phase with full loading and the ship's experience time of this environment was 3.105 years. Based on the inspections of the lug plate and calculated fatigue damages it can be concluded that Q8 Shell and Solid20W models cannot predict the fatigue damage correctly. Solid8W model has the best potential because the damage level of it was below 1. However, if the Solid8W damage would be calculated with 20-year design life the calculated damage would be over 1. The damages should also be calculated to other conditions to cover the whole history of conversion project. In terms of fatigue life, the Q8 Shell model and Solid20W models withstand the environmental loads less than 10 years at HS3. The Solid8W has over 30 years and Solid8W BR over 100 years fatigue life. At HS4, Q8 Shell model and Solid20W models has fatigue life less than 2 years. The

Solid8W model has 4 years and Solid8W BR has almost 11 years fatigue life. Longer fatigue life can be acquired with solid models and in that sense results are in line with the Wang's (2008) study. He also obtained very low fatigue lives on same hot spot locations. None of the models meet 25 years design requirement for FPSO. The conservatism of numerical analysis disappears with Solid8W and Solid8W BR models at HS3. Both models indicate higher fatigue life than 20 years, which was the case FPSOs' sailing time. On the other hand, none of the models can predict the fatigue life more than 11 years in HS4, which is in contradiction with inspections onboard the case ship.

The different weld corner representation changes the peak stress location, extension and magnitude. The Solid20W model without weld corner elements is the easiest to mesh with hex elements, but it gives unrealistic peak stress locations. Therefore, Solid20W model is not useful. The next easiest model to mesh is the Solid20W Tetra model, which has two tetra elements at the weld corner. It gives right peak stress location at the weld corner, but the vastness of peak stress area is affected by lug plate's back face weld. The Solid20W Wedge model, which take the most time to mesh of Solid20W models shows the best agreement with Solid8W model on the peak stress location and the vastness of peak stress areas. In this sense the Solid20W Wedge model should be the best of Solid20W models.

A lug plate is welded on the sides to a webframe leaving physical gap between the webframe and the lug plate. A gap is modeled with unconnected nodes when the forces are transformed only through the weld elements. The gap does not affect either to surface stress or structural hot spot response remarkably. Result of the gap effect is in line with Wang's (2008) study. Open question is, how much the gap would affect to results if the gap is modeled as it physically appears and how much the gap distance affects the results. However, more realistic gap representation would make meshing much more complicated and it is not even possible with sparse mesh and thus left out from this study.

The structural hot spot stresses calculated by extrapolation method deviate between different models. The scatter of the results is a vaster than in the IISC report (Horn et al. 2009). However, they did not study the lug plate connection. The Q8 Shell model shows highest stress compared to other models at HS3. The Solid20W Tetra model has lower hot spot stress compared to Solid20W Wedge model. The lowest hot spot stress is in Solid8W model. At HS4 hot spot stress results of Solid20W models are vice versa. Also

the Solid20W Tetra model has highest hot spot stress. The second highest hot spot stress is in Q8 Shell model. The difference between Solid20W models at HS3 and HS4 can be partly explained by different stress ROPs. The mesh size deviates between models at HS4. The quadratic curve fitting should compensate the deviation, but in this case it affects to hot spot stresses. Thus extrapolated structural hot spot stresses are not comparable at HS4. Also one may argue that in the Solid8W model the stress gradient is not properly captured. In the Solid8W model the stresses are extrapolated straight on the stress ROPs and the quadratic curve fitting is not used. However, the idea behind structural hot spot stress is to capture the structural stress gradient due to structural change not the stress peak. The stress peak effect is included in *S-N* curve. In order to capture the stress peak correctly one should use notch stress approach. The convergence study should be made in order to ensure if the Solid8W model gives “true” extrapolated stress result. Also the extrapolation method could be questioned. It is hard to distinguish is the hot spot location on free edge more closer to extrapolation case (a) or (b) in Figure 3.

The hot spot stresses calculated by through thickness linearization deviate a lot compared to surface extrapolated hot spot stresses in case of Q8 Shell model and Solid8W model. Result is in contradiction to fact, that hot spot stress should be same regardless of derivation technique (e.g. Fricke 2015). However, the thickness linearization is performed at the weld toe on the edge of the webframe, where weld goes around the lug plate. Thus the weld affects from two directions and functionality of linearization method could be questioned. The thickness linearized stress field is an approximation and not based on physical condition of stress field at the weld. This might lead to inaccurate through thickness stress linearization and thus bending and membrane stresses. With sparse mesh the determination of bending stress by integration leads to inaccurate bending stress. Therefore, the linearized stress field may as well be approximated with ordinary least square method to give estimation of bending and membrane stress in case of sparse mesh. To confirm realistic membrane and bending stresses the denser solid model should be investigated.

All the solid models show bending dominant behavior at the weld toe and the Q8 Shell model shows membrane dominant behavior. The Q8 Shell model cannot describe local bending at the hot spot. The reason for this is probably the offset element, which is modeled according to DNV guidelines. The behavior of the models starts to be consistent in terms of bending and membrane stresses, when the stresses are studied farther than $1t$

location from weld toe. Solid models with correct weld geometry representations give more accurate results at the hot spot. It can be concluded that the lug plate has high local bending at the weld toe and dense solid models are able to describe this behavior.

Bending reduced extrapolated hot spot stresses are in good agreement between solid models at HS3. Shell model differs from solid models due to wrong bending behavior at hot spot. Consistency between solid models' hot spot stresses is partly due to thickness linearized stresses at stress ROPs. This arise the question should the extrapolation be calculated based on thickness linearized stresses and $S-N$ curve tuned to correspond these. The full-scale model test should be carried out to investigate this possibility more.

Lug plate is very typical structure in longitudinal connection to webframe. Experiences have shown that fatigue strength of the lug plate should not be problem at least in double bottom area. However, rule based shell element modeling has shown fatigue damage of the lug plate in multiple projects. This thesis confirms those experiences that shell models are too conservative and shows damage even if inspections onboard ship has not confirmed fatigue cracks. A dense solid model (Solid8W) gives more realistic result compared to experience, but still shows damage in relatively short time. Based on this it seems that fatigue assessment procedure has too much conservatism. Studying other sources of conservatism has been left out of this thesis.

7 Conclusions

This thesis studied the fatigue assessment of the lug plate connection on real case FPSO conversion project. The experience has shown that the lug plate should not be problematic in terms of fatigue, but numerical analysis with shell models suggests otherwise. This thesis studies the sources of conservatism in fatigue stress analysis. The main focus was on the stress state analysis of the lug plate with solid FE-models and comparing results to shell models, which represent standard modeling technique in ship design. The stress response was studied in principal stress, structural hot spot stress acquired by extrapolation technique and thickness linearization levels. Also the membrane and bending stresses were studied at the hot spot location. In addition, the fatigue damage analysis of the lug plate connection was carried out.

The solid modeling technique requires a lot more time to prepare the geometric model and generating the mesh. However, the solid models can more realistically represent the weld connection on the lug plate. The effects of more realistic weld representation can be seen from deformation and stress results. Two element layers made the model stiffer compared to shell and denser solid model. The tetra element weld corner representation made the model more flexible compared to wedge weld corner at the hot spot location.

Results of the extrapolated stresses indicate that dense solid models have the lowest stress response on both hot spot locations and therefore dense models are the least conservative. The structural hot spot stresses of the shell and solid models with two element layers (Solid20W models) were about on the same level. The deviation between dense and Solid20W models is due the higher stiffness of the Solid20W models. The difference between Solid20W models results at HS3 and HS4 can partly be explained by differences in mesh size. Thickness linearization method was found unsuitable in lug plate connection. The reason for this is the fact that weld goes around the lug plate and affects to thickness linearization from side.

The bending and membrane stress of shell model deviated from solid models at hot spot location. The shell model was not able to capture bending dominant behavior at hot spot location. Wrong behavior is due to weld representation with offset element. However, the bending behavior of all models on webframe in way of lug plate is very similar and the models mainly differ at the weld toe. The result indicates that bending reduction of hot spot stresses is justified.

The damage calculation SRF's based on stresses calculated from extrapolated technique. The damage calculations of shell and Solid20W models showed that they cannot predict the fatigue damage properly. The more densely meshed Solid8W models give more realistic results, but would not withstand the whole design life of FPSO even if the bending reduction is used.

The solid models had shown to be better to describe the stress state of the lug plate connection. The results of Solid8W models are more in line with the observations of the FPSO ship where the fatigue damage did not occur. However, the expected design life of lug plate is shorter than required for FPSOs. Even though the solid models are more time consuming to construct, the results of damage calculation and stress response calculation had shown that the fatigue analysis of lug plate connection should be done with dense solid models taking into account the correct weld geometry.

8 Future work and recommendations

The solid modeling is time consuming. Thus the efficient way of implementing and improving solid meshing techniques should be studied. Also full tetra meshed models should be studied. Tetra meshing is much faster, because the commercial FE programs have good automated meshing tools for tetra meshing. For hex meshing the HyperMesh program have better tools compared to other FE programs and the implementation process of HyperMesh could be improved by in-house design process.

The solid model size should be studied. The Solid8W model does not cover the whole lug plate and the stiffener is modeled with beam and shell elements. This leaves open is the stiffness of longitudinal taken into account properly and will it affect to structural hot spot stress and fatigue damage.

Different models gave very large scatter in structural hot spot stress. The denser meshes should be studied to see if convergence of hot spot stresses could be obtained. Structural hot spot stresses from bending reduced extrapolation technique gave the smallest scatter. The clear instructions how and when the bending reduction could be applied should be studied in more detailed. The results should be verified against notch stress method in terms of fatigue damage. Also full-scale model test would give better understanding about the results.

References

- American Bureau of Shipping., 2014. Guide for Spectral-Based Fatigue Analysis for Floating Production, Storage and Offloading (FPSO) Installations. 3rd ed. American Bureau of Shipping.
- American Bureau of Shipping., 2013. Floating Production Installations. 3rd ed. Houston: American Bureau of Shipping, July 2014,.
- American Bureau of Shipping., 2003. Fatigue assessment of offshore structures. February 2014 ed. Houston: ABS, April,.
- Aygül, M., 2012. Fatigue Analysis of Welded Structures Using the Finite Element Method. ISBN 1652-9146.
- Chattopadhyay, A., 2011. Stress analysis and fatigue of welded structures. *Welding in the World*, vol. 55, no. 7-8, pp. 2-21 ISSN 0043-2288.
- Cook, R.D., 2001. Concepts and applications of finite element analysis, fourth edition. New York, N.Y.: Wiley ISBN 0-471-35605-0.
- Det Norske Veritas., 2012. Fatigue methodology of offshore ships. RP-C206 ed. DNV, October,.
- Det Norske Veritas., 2011. Fatigue design of offshore steel structures. RP-C203 ed. DNV, October,.
- Det Norske Veritas., 2010. Fatigue Assessment of Ship Structures. Classification notes No. 30.7 ed. DNV, June,.
- DNV GL., 2015. Class guideline DNVGL-CG-0127 Finite element analysis. DNV GL, October 2015,.
- Dong, P., 2001. A structural stress definition and numerical implementation for fatigue analysis of welded joints. *International Journal of Fatigue*, vol. 23, no. 10, pp. 865-876 ISSN 0142-1123. DOI 10.1016/S0142-1123(01)00055-X.
- European Committee For Standardization., 1992. Eurocode 3: Design of Steel Structures. Belgium: CEN.
- Fricke, W., 2015. Recent developments and future challenges in fatigue strength assessment of welded joints. *Proceedings of the Institution of Mechanical Engineers; Part C; Journal of Mechanical Engineering Science*, vol. 229, no. 7, pp. 1224-1239 ISSN 0954-4062. DOI 10.1177/0954406214550015.
- Fricke, W., 2003. Fatigue analysis of welded joints: state of development. *Marine Structures*, vol. 16, no. 3, pp. 185-200 ISSN 0951-8339. DOI 10.1016/S0951-8339(02)00075-8.

Fricke, W., 2002. Recommended Hot-Spot Analysis Procedure for Structural Details of Ships and FPSOs Based on Round-Robin FE Analyses. *International Journal of Offshore and Polar Engineering*, vol. 12, no. 1, pp. 40-47 ISSN 1053-5381.

Fricke, W. and Kahl, A., 2005. Comparison of different structural stress approaches for fatigue assessment of welded ship structures. *Marine Structures*, vol. 18, no. 7-8, pp. 473-488 ISSN 0951-8339. DOI 10.1016/j.marstruc.2006.02.001.

Fricke, W. and Paetzold, H., 2010. Full-scale fatigue tests of ship structures to validate the S-N approaches for fatigue strength assessment. *Marine Structures*, vol. 23, no. 1, pp. 115-130 ISSN 0951-8339. DOI 10.1016/j.marstruc.2010.01.004.

Fricke, W. and Paetzoldt, H., 1995. Fatigue strength assessment of scallops —an example for the application of nominal and local stress approaches. *Marine Structures*, vol. 8, no. 4, pp. 423-447 ISSN 0951-8339. DOI 10.1016/0951-8339(94)00029-R.

Fricke, W., Doerk, O. and Weissenbord, C., 2003. Comparison of different calculation methods for structural stresses at welded joints. *International Journal of Fatigue*, vol. 25, no. 5, pp. 359-369 ISSN 0142-1123. DOI 10.1016/S0142-1123(02)00167-6.

Fricke, W., Von Lileienfeld-Toal, A. and Paetzoldt, H., 2012. Fatigue strength investigations of welded details of stiffened plate structures in steel ships. *International Journal of Fatigue*, vol. 34, no. 1, pp. 17-26 ISSN 0142-1123.

Goyal, R.K., 2015. A robust and efficient model for fatigue life prediction of welded structures. Doctor of Philosophy ed. Waterloo, Ontario, Canada: Mechanical Engineering, University of Waterloo.

Hobbacher, A., 2008. Recommendations for Fatigue Design of Welded Joints and Components. Doc. XIII-2151r4-07/XV-1254r4-07 ed. Paris, France: The International Institute of Weldings, October,.

Horn, A.M., Aihara,S., Andersen,M., Biot,M., Bohlmann,B., van der Cammen,J., Choi,B.K., Garbatov,Y., Mishra,B., Qian,X., Remes,H., Ringsberg,J., Samanta,A., Wang,D.and Zhang,S., 2012. ISSC committee III.2 - Fatigue and fracture. ISBN 3-87700-131-9.

Horn, A.M., Andersen,M.R., Biot,M., Bohlmann,B.M., S., Kozak,J., Osawa,N., Jang, Y.S.,Remes, H., Ringsberg,J.and van der Cammen,J., 2009. ISSC committee III.2 - Fatigue and fracture. ISBN 89-954730-1-0.

Hughes, O.F. and Paik, J.K., 2010. Ship Structural Analysis and Design. Society of Naval Architects and Marine Engineers (SNAME) ISBN 978-0-939773-78-3.

Kang, S.W., Kim, W.S. and Paik, Y.M., 2002. Fatigue Strength of Fillet Welded Steel Structure Under Out-of-plane Bending Load. *International Journal of Korean Welding Society*, vol. 2, pp. 33-39 ISSN 1598-1177.

Karadeniz, H., 2013. Stochastic analysis of offshore steel structures : an analytical appraisal. Springer London ISBN 1-84996-189-1.

Kukkanen, T., 1996. Spectral fatigue analysis for ship structures. Licentiate ed. Helsinki: Helsinki University of Technology, Ship Laboratory, 20.05,.

Le Cotty, A. and Selhorst, M., 2003. New Build Generic Large FPSO, vol. OTC 15311, no. Offshore Technology Conference pp. 14.04.2016. Available from: http://theplatforma.org/files/New_build_generic_large_FPSO.pdf.

Lewis, E.V., 1988. Principles of Naval Architecture: Stability and Strength. Volume 1. Second Revision. The Society of Naval Architects and Marine Engineers ISBN 0-939773-00-7.

Lindemark, T., Lotsberg, I., Kang, J.-., Kim, K.-. and Oma, N. Fatigue capacity of stiffener to web frame connections Anonymous *Proceedings of the International Conference on Offshore Mechanics and Arctic Engineering - OMAE*, 2009.

Lloyd's Register., 2012. Structural Design Assessment - Primary Structure of Ro-Ro Ships. 1st ed. London: Lloyd's Register, March,.

Lotsberg, I., 2006. Fatigue design of plated structures using finite element analysis. *Ships and Offshore Structures*, vol. 1, no. 1, pp. 45-54 ISSN 1744-5302. DOI 10.1533/saos.2005.0006.

Lotsberg, I., 2005. Fatigue capacity of side longitudinals in floating structures. *Marine Structures*, vol. 18, no. 1, pp. 25-42 ISSN 0951-8339. DOI 10.1016/j.marstruc.2005.08.002.

Lotsberg, I., 2007. Recent advances on fatigue limit state design for FPSOs. *Ships and Offshore Structures*, vol. 2, no. 1, pp. 49-68 ISSN 1744-5302.

Matusiak, J., 2013. Dynamics of a rigid ship. Aalto University, School of Engineering, Department of Applied Mechanics, Marine Technology ISBN 952-60-5204-8.

Milella, P.P., 2013. Fatigue and corrosion in metals. Milan: Springer ISBN 9788847023369.

Niemi, E., Fricke, W. and Maddox, S.J., 2006. Fatigue analysis of welded components : designer's guide to the structural hot-spot stress approach (IIW-1430-00). Cambridge : Boca Raton (FL) : Woodhead Publishing ; CRC Press ISBN 1-84569-124-5 (Woodhead).

Osawa, N., Hashimoto, K., Sawamura, J., Nakai, T. and Suzuki, S., 2007. Study on shell-solid coupling FE analysis for fatigue assessment of ship structure. *Marine Structures*, vol. 20, no. 3, pp. 143-163 ISSN 0951-8339. DOI 10.1016/j.marstruc.2007.04.002.

Poutiainen, I., Tanskanen, P. and Marquis, G., 2004. Finite element methods for structural hot spot stress determination—a comparison of procedures. *International Journal of Fatigue*, 11, vol. 26, no. 11, pp. 1147-1157 ISSN 0142-1123. DOI <http://dx.doi.org.libproxy.aalto.fi/10.1016/j.ijfatigue.2004.04.003>.

Prayer, H.G. and Fricke, W., 1994. Rational Dimensioning and Analysis of Complex Ship Structures. *SNAME Transactions*, vol. 102, pp. 395-417.

Radaj, D., Sonsino, C.M. and Fricke, W., 2009. Recent developments in local concepts of fatigue assessment of welded joints. *International Journal of Fatigue*, vol. 31, no. 1, pp. 2-11 ISSN 0142-1123. DOI 10.1016/j.ijfatigue.2008.05.019.

Radaj, D., 1990. Design and Analysis of Fatigue Resistant Welded Structures. Woodhead Publishing ISBN 1-85573-004-9.

Shimamura, Y., 2002. FPSO/FSO: State of the art. *Journal of Marine Science and Technology*, Sep 2002, vol. 7, no. 2, pp. 59-70 ProQuest Aquatic Science Collection, ProQuest Atmospheric Science Collection, ProQuest Environmental Science Collection. ISSN 09484280. DOI <http://dx.doi.org/10.1007/s007730200013>.

Siemens., 2015. NX Nastran User's Guide.

Sonsino, C.M., Fricke, W., de Bruyne, F., Hoppe, A., Ahmadi, A. and Zhang, G., 2012. Notch stress concepts for the fatigue assessment of welded joints – Background and applications. *International Journal of Fatigue*, 1, vol. 34, no. 1, pp. 2-16 ISSN 0142-1123. DOI <http://dx.doi.org.libproxy.aalto.fi/10.1016/j.ijfatigue.2010.04.011>.

Tran Nguyen, K., Garbatov, Y. and Guedes Soares, C., 2012. Fatigue damage assessment of corroded oil tanker details based on global and local stress approaches. *International Journal of Fatigue*, vol. 43, pp. 197-206 ISSN 0142-1123. DOI 10.1016/j.ijfatigue.2012.04.004.

Wang, Z., 2008. Fatigue Behavior and Failure Assessment of Plate Connections in Ship Shaped Structures. Doctoral Dissertation ed. National University of Singapore.

List of appendices

Appendix 1. Wave scatter. 1 page.

Appendix 2. Deformations of different models. 3 pages.

Appendix 1 Wave scatter

	Tz (s)	1.9	2.7	3.4	4.2	5.0	5.7	6.5	7.3	8.0	8.8	9.6	10.3	11.1	11.9	12.6	13.4	14.1	14.9	15.7	16.4	17.2	
Hs (m)																							
0.5		1	150	1073	1880	2967	2989	2345	1689	838	422	242	95	57	37	27	11	10	3	3	0	0	14819
1.5		0	21	1224	4615	6815	8706	10387	8343	5820	3863	2331	1152	561	348	225	80	62	29	20	12	5	54599
2.5		0	0	8	489	2923	4774	5389	6246	5820	4558	3050	2028	1085	616	337	128	112	25	23	9	5	37565
3.5		0	0	0	8	256	1510	3169	3680	3868	3481	2723	1665	1010	656	360	148	106	30	14	4	3	22891
4.5		0	0	0	0	6	117	919	1807	2492	2237	1727	1204	809	462	247	109	97	15	10	1	0	12259
5.5		0	0	0	0	0	4	117	511	1157	1561	1243	754	421	311	182	74	49	6	3	0	2	6395
6.5		0	0	0	0	0	0	11	57	288	750	986	554	251	181	100	64	34	5	3	0	0	3244
7.5		0	0	0	0	0	0	0	6	42	240	485	536	230	113	50	51	33	0	0	0	0	1736
8.5		0	0	0	0	0	0	0	0	5	39	125	348	162	96	30	24	19	2	0	0	0	850
9.5		0	0	0	0	0	0	0	0	0	3	29	114	129	75	27	16	9	0	1	0	0	403
10.5		0	0	0	0	0	0	0	0	0	0	5	21	61	39	17	13	9	0	0	0	0	165
11.5		0	0	0	0	0	0	0	0	0	0	0	4	25	11	9	4	2	0	0	0	0	55
12.5		0	0	0	0	0	0	0	0	0	0	0	0	2	5	7	4	0	0	0	0	0	18
13.5		0	0	0	0	0	0	0	0	0	0	0	0	2	2	5	2	0	0	0	0	0	11
14.5		0	0	0	0	0	0	0	0	0	0	0	0	0	1	0	2	0	0	0	0	0	3
15.5		0	0	0	0	0	0	0	0	0	0	0	0	0	0	0	0	0	0	0	0	0	0
16.5		0	0	0	0	0	0	0	0	0	0	0	0	0	0	0	1	0	0	0	0	0	1
		1	171	2305	6992	12967	18080	22287	22299	20330	17154	12926	8450	4775	2853	1623	731	542	115	77	26	15	15864

Appendix 2 Deformations of different models

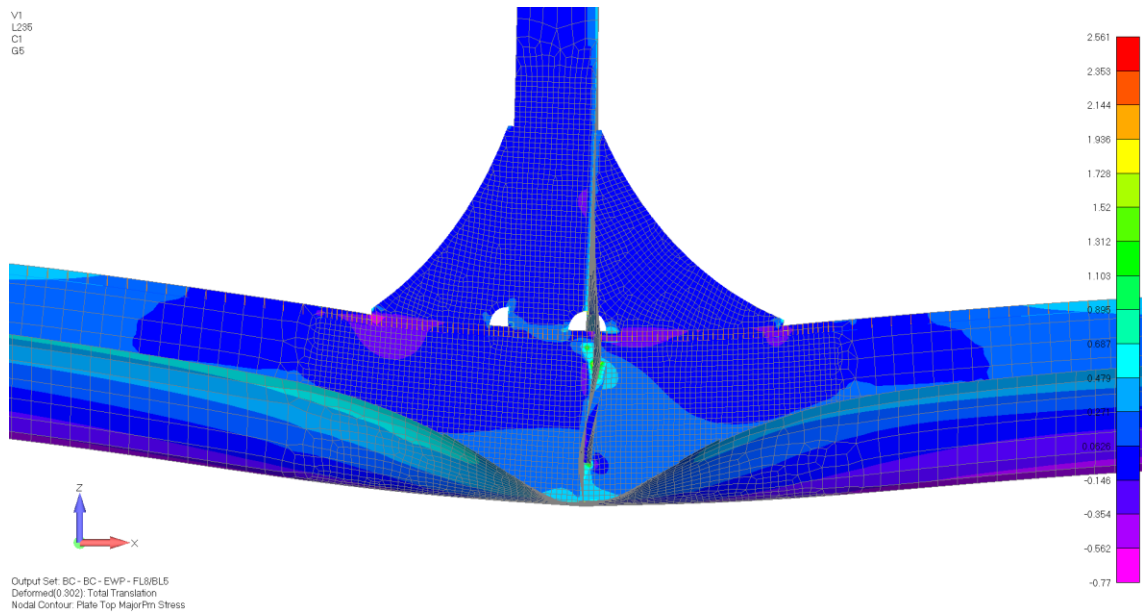


Figure A2- 1 Q8 Shell

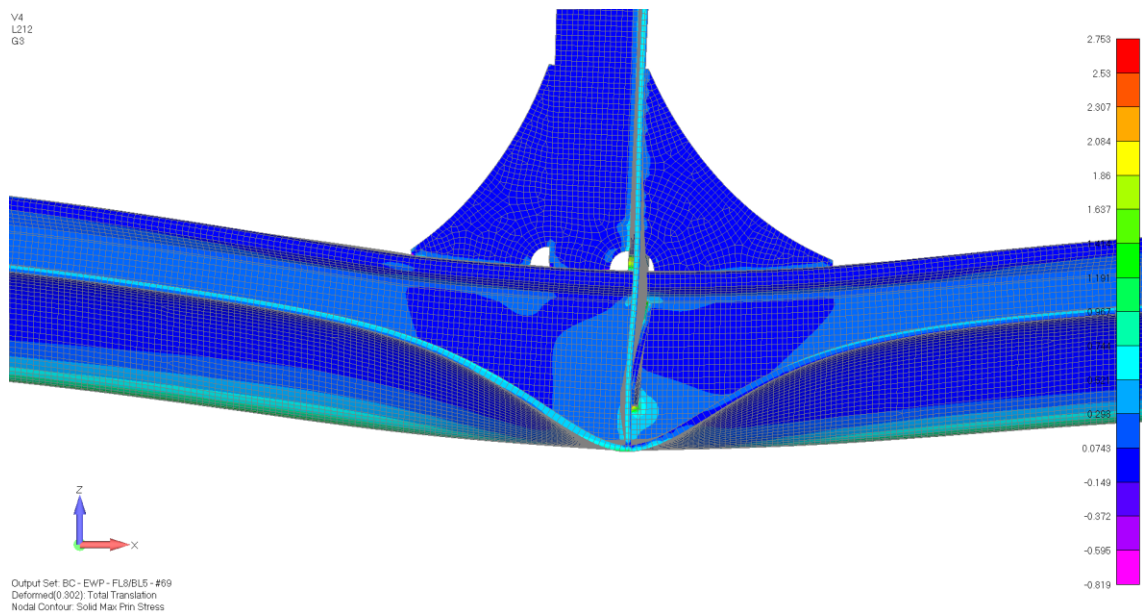


Figure A2 - 2 Solid20 Wedge.

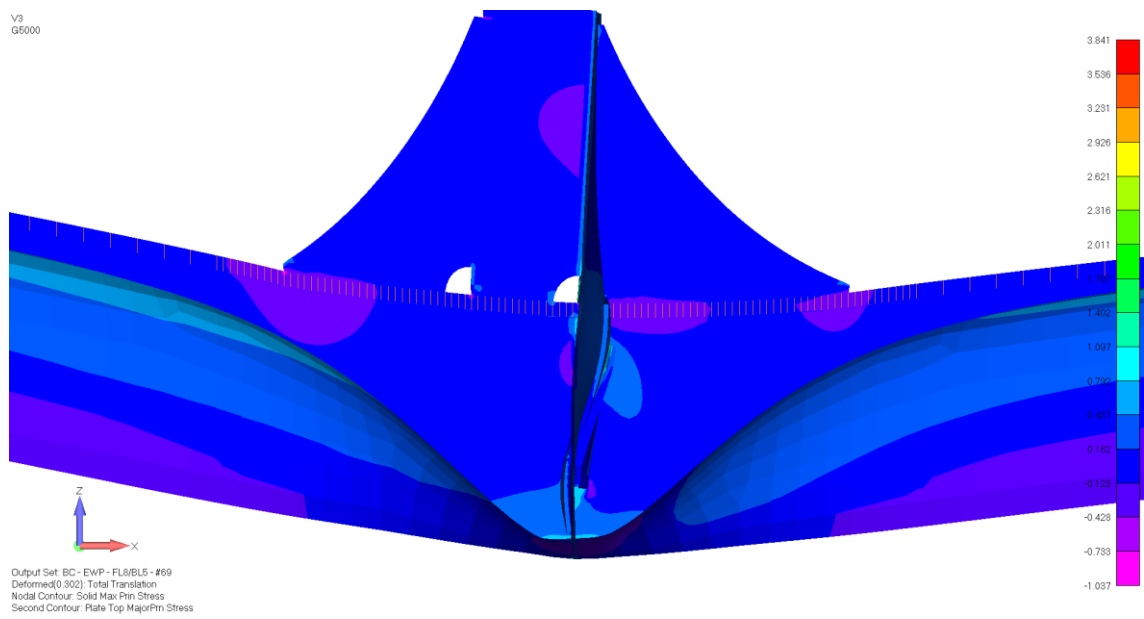


Figure A2- 3 Solid8W

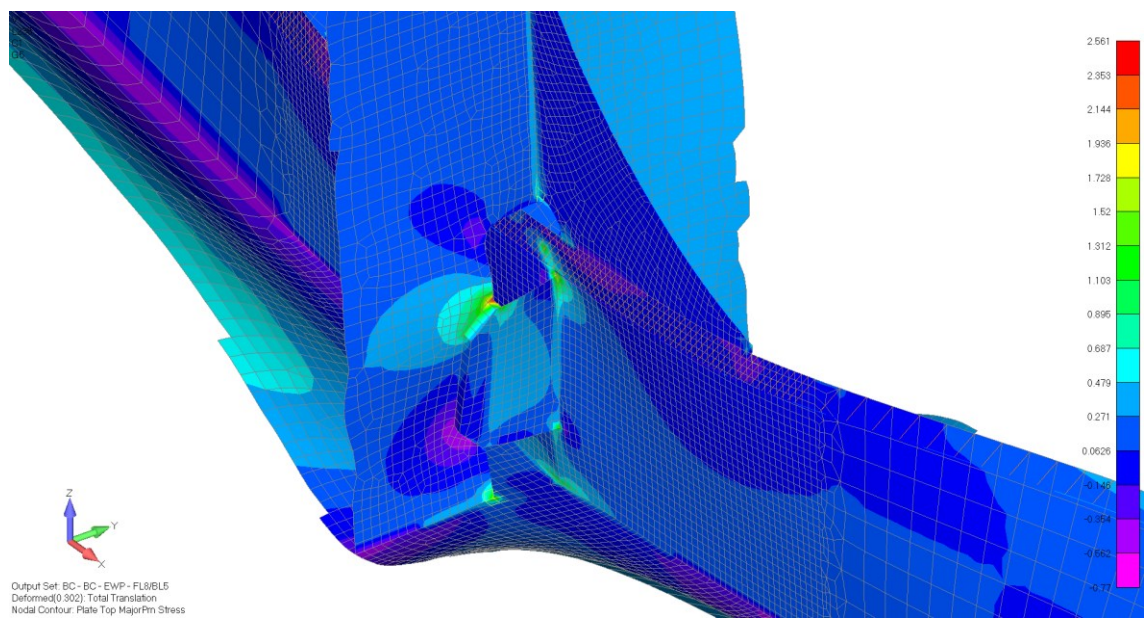


Figure A2- 4 Q8 Shell

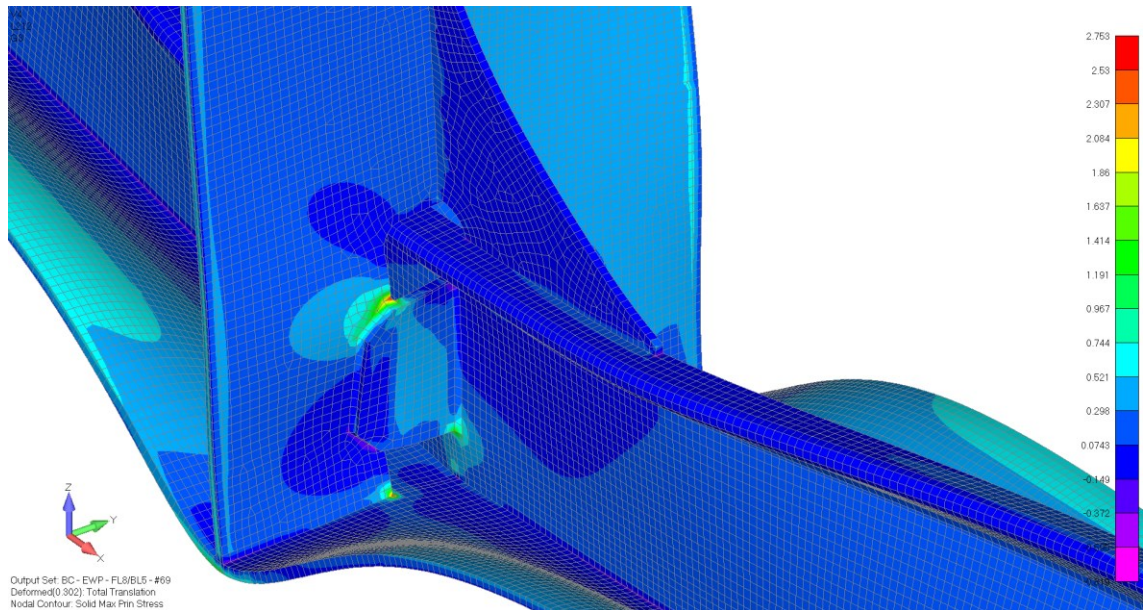


Figure A2- 5 Solid20W Wedge

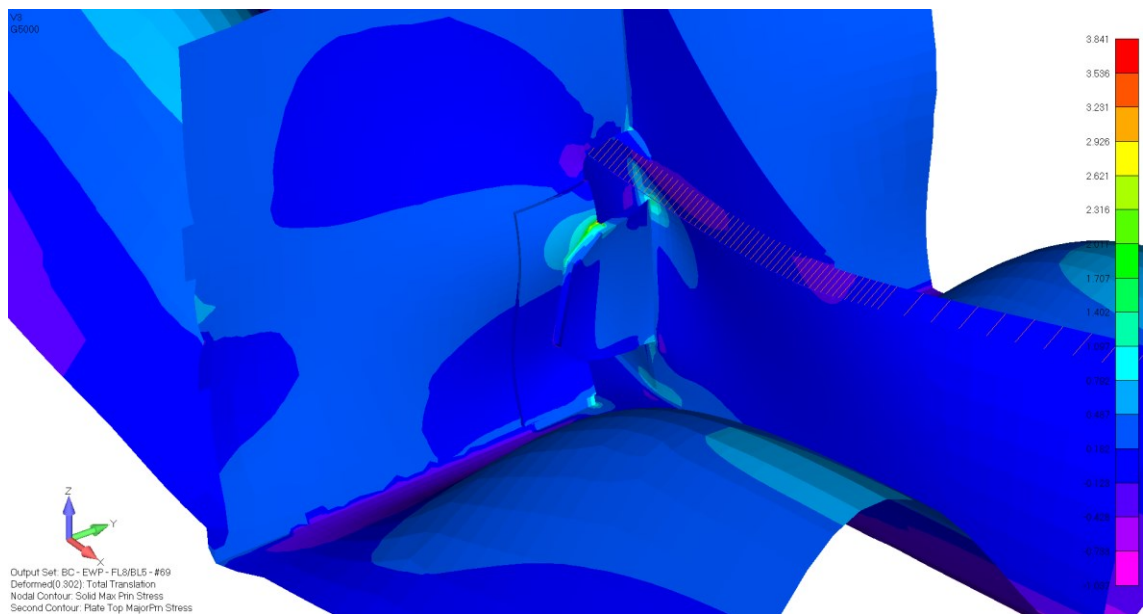


Figure A2- 6 Solid8W